Applied Energy 426 (2026) 128574

Contents lists available at ScienceDirect

Applied Energy

journal homepage: www.elsevier.com/locate/apen

# Long-term deployment of marine current turbines: a review of biofouling effects on performance degradation, mitigation strategies and techno-economic impacts

Luana Gurnari[a,*], Pasquale Filianoti[b], Domenico Coiro[c], Marco Torresi[a], Sergio Mario Camporeale[a]

[a] Polytechnic of Bari, Via Amendola 126/b, Bari, 70126, Italy
[b] University Mediterranea of Reggio Calabria, Via Zehender, 1, Reggio Calabria, 89128, Italy
[c] University of Naples Federico II, C.so Umberto I, 40, Naples, 80138, Italy

## HIGHLIGHTS

- Review of biofouling effects on Marine Current Turbines, with focus on long-term performance degradation.
- Critical overview of scientific literature on hydrodynamic, operational and techno-economic impacts of fouling.
- Discussion of CFD approaches, antifouling strategies and site-specific experimental methodologies.
- Integrated perspective linking biofouling evolution, turbine efficiency losses and maintenance planning.

## GRAPHICAL ABSTRACT

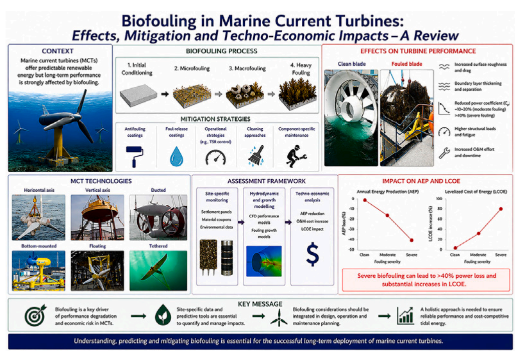


## ARTICLE INFO

*Keywords:*
Tidal energy
Marine current turbines
Biofouling
Performance degradation
Antifouling strategies
Predictive modelling
AEP
LCOE

## ABSTRACT

Marine current turbines (MCTs) are a promising technology for predictable renewable energy generation, but their long-term performance is significantly affected by the harsh marine environment. Among the various degradation mechanisms, biofouling is one of the most critical, as it increases surface roughness, modifies hydrodynamic loads, reduces energy conversion efficiency, and raises operation and maintenance costs. This review critically examines the effects of biofouling on MCT performance by integrating hydrodynamic, biological, operational, and techno-economic perspectives. Existing experimental, numerical, and field studies indicate that moderate biofouling typically reduces the power coefficient by 10–20%, while severe natural colonisation may lead to power losses exceeding 40%, with the magnitude of degradation depending on fouling morphology, turbine configuration, installation conditions, and operating strategy. The effectiveness and limitations of current mitigation approaches, including antifouling and foul-release coatings, adaptive tip-speed-ratio control, cleaning schedules, and component-specific maintenance strategies, are systematically discussed. A key contribution of this review is the identification of the gap between site-specific biofouling observations, predictive growth modelling, and turbine performance assessment. To address this limitation, an integrated framework is proposed that combines local biofouling monitoring, hydrodynamic modelling, and techno-economic indicators to support

* Corresponding author.
*Email addresses:* luana.gurnari@poliba.it (L. Gurnari), filianoti@unirc.it (P. Filianoti), coiro@unina.it (D. Coiro), marco.torresi@poliba.it (M. Torresi), sergio.camporeale@poliba.it (S.M. Camporeale).

https://doi.org/10.1016/j.apenergy.2026.128574
Received 21 May 2026; Received in revised form 20 July 2026; Accepted 27 July 2026
Available online 6 August 2026

lifecycle performance assessment. The analysis highlights that biofouling should be considered not only as a surface degradation phenomenon but also as a key lifecycle driver influencing turbine design, maintenance planning, annual energy production, and the economic viability of tidal energy systems.

**Nomenclature**

| | |
|---|---|
| ADCP | Acoustic Doppler Current Profiler |
| AEP | Annual Energy Production |
| BEMT | Blade Element Momentum Theory |
| CAPEX | Capital Expenditure |
| CFD | Computational Fluid Dynamics |
| CP | Power Coefficient |
| CT | Thrust Coefficient |
| DREA | Defence Research Establishment Atlantic |
| EIA | Environmental Impact Assessment |
| GEM | Tethered marine current turbine platform (Generatore Elettrico Marino) |
| HATT | Horizontal Axis Tidal Turbine |
| LCOE | Levelized Cost Of Energy |
| LES | Large Eddy Simulation |
| MCT | Marine Current Turbine |
| ML | Machine Learning |
| MRF | Multiple Reference Frame |
| OPEX | Operational Expenditure |
| PMG | Permanent Magnet Generator |
| RANS | Reynolds-Averaged Navier–Stokes |
| SPC | Self-Polishing Copolymer |
| SST | Shear Stress Transport |
| TSR | Tip-Speed Ratio |
| TCEC | Tidal Current Energy Converter |
| TCPGF | Tidal Current Power Generation Farm |
| URANS | Unsteady Reynolds-Averaged Navier–Stokes |
| VATT | Vertical Axis Tidal Turbine |

## 1. Introduction

The increasing demand for clean and renewable energy sources has stimulated growing interest in ocean energy, as the oceans cover about 70% of the Earth's surface [1]. Ocean energy includes tidal currents, waves, and temperature and salinity gradients, each characterised by different levels of technological maturity and resource potential. Among these resources, tidal energy is particularly attractive because of its high predictability, sustainability, and relatively low environmental impact. Tidal current systems convert the kinetic energy of flowing water into electricity through underwater energy converters. Although the theoretical global potential is considerable, its practical exploitation remains strongly site-dependent [2]. According to [3], estimates of the exploitable resource vary depending on the assumptions adopted. The theoretical hydrokinetic potential of ocean and tidal currents has been estimated at approximately 7800 TWh per year (890 GW) [4], while the total energy available from global tides is about 3000 GW [5,6]. However, only a fraction of this resource can be effectively exploited because tidal energy is concentrated in locations characterised by favourable bathymetry and strong current acceleration, such as narrow straits and shallow coastal areas. In Europe alone, 106 sites with high tidal-stream potential have been identified, corresponding to an estimated annual production of about 48 TWh [2].

In recent decades, there has been considerable progress in the development of Tidal Current Energy Converters (TCECs). Several prototypes have been tested, and some have been deployed commercially. Notable examples include the MeyGen project in Scotland, the largest operating tidal power plant in the world, and the Sabella D10 turbine in France, which enables long-term grid connection. These projects demonstrate both technological advances and the remaining challenges in scaling up tidal energy production. Despite these advances, the technology still faces numerous challenges, including high installation costs, long service life in severe marine environments, and the need for efficient energy conversion systems. Harsh marine conditions present various obstacles, such as the formation of biofouling, which reduces performance and increases maintenance requirements, and corrosion caused by prolonged deployment in salt water. Addressing these environmental factors is crucial to ensure the long-term reliability and economic feasibility of tidal energy systems.

Several review papers have contributed significantly to the development of tidal energy research by addressing different aspects of the technology, including hydrokinetic energy conversion, turbine design, resource assessment, farm planning, and wake modelling. Khan et al. [7] presented one of the earliest and most comprehensive reviews of hydrokinetic energy conversion technologies, discussing turbine configurations, flow optimisation, installation strategies, and emerging concepts such as diffuser-augmented devices, piezoelectric systems, biomimetic technologies, and vortex-induced vibration energy converters. Their review also highlighted the potential application of hydrokinetic turbines in rivers, artificial channels, irrigation canals, tidal currents, and ocean currents, providing a comprehensive overview of the technological trends that characterised the early development of the sector. O'Rourke et al. [8] reviewed the technological status of tidal energy systems, describing both tidal barrages and tidal current turbines and discussing their respective advantages and limitations. Their work also emphasised the importance of supportive policy frameworks, comprehensive resource assessment, and appropriate economic incentives to accelerate the commercial deployment of tidal energy technologies.

More recent reviews have focused on increasingly specialised topics. Zhibin et al. [9] analysed the latest developments in large-scale Marine Current Turbine (MCT) technologies, with particular emphasis on megawatt-class horizontal-axis and floating turbines. Zhixue et al. [10] reviewed planning methodologies for Tidal Current Power Generation Farms, covering site selection, turbine layout optimisation, environmental impact assessment, Computational Fluid Dynamics (CFD), optimisation algorithms, and the integration of Levelised Cost of Energy (LCOE) into farm planning. More recently, Xiaodong et al. [11] summarised the current understanding of wake characteristics in Horizontal Axis Tidal Turbines (HATTs), highlighting recent advances in both numerical and experimental investigations together with the remaining knowledge gaps in wake prediction. Collectively, these reviews have substantially advanced the understanding of tidal energy systems. However, their primary focus has been on turbine technologies, resource assessment, farm optimisation, wake dynamics, and deployment strategies, whereas the long-term effects of biofouling have generally received only limited attention. In particular, the interaction between biological colonisation, hydrodynamic performance degradation, maintenance planning, and lifecycle techno-economic assessment has not yet been addressed within a unified framework.

The present review addresses this gap by focusing specifically on biofouling as a key driver of long-term performance degradation in Marine Current Turbines. Unlike mature offshore sectors such as shipping and offshore oil and gas, where biofouling has been extensively investigated, knowledge regarding tidal turbines remains fragmented and is largely based on laboratory studies or short-term deployments, with limited evidence from full-scale operating systems. Accordingly, this review not only summarises the current state of knowledge but also critically analyses the relationships between biofouling development, hydrodynamic performance degradation, maintenance strategies, and lifecycle techno-economic impacts. Particular attention is devoted to identifying transferable methodologies from related offshore sectors, highlighting current research gaps, and discussing future research priorities required to develop predictive, lifecycle-oriented biofouling assessment frameworks for Marine Current Turbines. This review integrates hydrodynamic, material, biological, operational, and environmental perspectives to assess the effects of long-term deployment on Marine Current Turbines. The overall objective is to demonstrate that biofouling should be regarded not simply as a surface degradation phenomenon but as a key lifecycle performance driver that influences turbine design, operation, maintenance planning, and economic viability. The paper is organised as follows. After a brief overview of the most relevant tidal energy technologies and pilot projects, Section 2 presents the latest advances in commercial and demonstration plants. Section 3 reviews the effects of biofouling on MCT performance, together with the associated degradation mechanisms and mitigation strategies. Finally, Section 5 summarises the main findings and outlines future research directions.

## 2. Pilot projects and commercial plants

Marine current turbines (MCTs) can be broadly classified as Horizontal Axis Tidal Turbines (HATTs) and Vertical Axis Tidal Turbines (VATTs). In several configurations, turbines are equipped with diffusers or shrouds to accelerate the incoming flow and enhance energy extraction. Studies on horizontal-axis turbines investigated the optimisation of diffuser geometry and shroud aerodynamic profiles, demonstrating the strong influence of duct shape on flow acceleration and turbine efficiency [12–14]. Numerical and experimental investigations further analysed diffuser-augmented hydrokinetic turbines through CFD simulations, laboratory-scale measurements, and optimisation procedures [15–17]. Broader review papers subsequently assessed diffuser-augmented turbine technologies and discussed their applicability to renewable energy systems [3,18,19]. Depending on the deployment strategy, tidal turbines may operate either as isolated devices or within tidal farms, where wake interactions and array optimisation become key design issues. Foundational theoretical studies analysed the maximum extractable power and the efficiency limits of turbine farms in channel flows [20,21], while subsequent investigations addressed turbine layout optimisation and resource assessment using coupled numerical approaches for tidal-stream farms [22,23].

HATTs are currently the dominant technological solution for commercial-scale tidal energy conversion owing to their high efficiency and technological maturity. Their hydrodynamic behaviour is strongly influenced by blade geometry, solidity, and pitch-control strategy. Fixed-pitch configurations are generally simpler and more robust, whereas variable-pitch turbines can better adapt to bidirectional tidal flows. Since turbine efficiency strongly depends on blade lift-to-drag ratio and boundary-layer behaviour, HATTs are particularly sensitive to biofouling-induced surface roughness and the associated hydrodynamic degradation during long-term deployment.

VATTs operate independently of the incoming flow direction and therefore do not require yaw mechanisms. Their aerodynamic behaviour has been extensively investigated using streamtube-based modelling approaches originally developed for vertical-axis wind turbines. Early studies established the theoretical foundations for Darrieus rotor analysis and streamtube methods for predicting turbine performance [24–26]. These approaches were subsequently extended to hydrokinetic applications, where numerical investigations analysed the performance of Darrieus-type rotors for low-head hydropower generation and assessed the influence of key geometric parameters on helical hydrokinetic turbine efficiency [27,28]. Early tidal energy applications based on the Voith–Schneider concept demonstrated the feasibility of vertical-axis configurations, although cyclic blade loading and torque fluctuations remain significant challenges [29]. Helical blade arrangements, such as the Gorlov rotor, can partially mitigate these unsteady effects [30,31]. Compared with HATTs, VATTs are generally more sensitive to the combined effects of surface roughness, dynamic stall, and unsteady hydrodynamic loading.

Support structures also play a crucial role in long-term deployment and maintenance strategies. Current tidal energy systems generally adopt gravity-based foundations, monopiles, piled jacket structures, or floating and tethered configurations. Bottom-mounted solutions provide high structural stability in energetic tidal environments, whereas floating and tethered systems facilitate installation and retrieval operations, particularly in deep-water applications. However, floating configurations introduce additional submerged components, including mooring systems, articulated joints, and floating supports, which are also exposed to marine growth and corrosion.

Several pilot and commercial projects have demonstrated the technical feasibility of tidal energy conversion in real marine conditions. Full-scale HATT deployments include MeyGen [32], SeaGen [33,34], Hammerfest [35], Sabella D10 [36], Verdant Power [37], and Orbital Marine Power [38,39]. These systems use various deployment strategies, including monopile, gravity-based, and floating configurations, and have provided operational experience regarding survivability, installation procedures, and maintenance requirements.

In particular, floating concepts such as Orbital Marine Power and tethered systems such as GEM/GEMSTAR have attracted increasing attention because they simplify retrieval operations and can potentially reduce maintenance costs during long-term deployment. Early developments of the GEM concept focused on optimising diffuser geometries for tethered horizontal-axis hydro turbines, highlighting the benefits of ducted configurations in improving energy extraction efficiency [14,15]. Subsequent studies addressed the full-scale development, deployment, and experimental validation of the GEM platform under real operating conditions, demonstrating the feasibility of tethered tidal-current systems for marine energy exploitation [40]. More recent work investigated the evolution of the GEMSTAR concept, including fixed-pitch rotor configurations controlled through permanent-magnet generator defluxing techniques to improve operational flexibility and system reliability [41].

Diffuser-augmented and shrouded turbines represent another important technological solution for increasing energy extraction. OpenHydro [42], Lunar Energy [43], and GEM/GEMSTAR [14,40] employ ducted configurations to accelerate the incoming flow and improve rotor performance. In these systems, however, marine growth may affect not only blade roughness but also the hydrodynamic behaviour of the duct, reducing flow acceleration and pressure recovery. Consequently, biofouling may also compromise the effectiveness of the augmentation system itself. VATT-based technologies have also been investigated through systems such as Kobold [3,44,45], Gorlov turbines [46,47], HydroQuest [48,49], and Blue Energy tidal fences [50]. These concepts benefit from yaw-independent operation and simplified drivetrain configurations, although their hydrodynamic response remains strongly influenced by cyclic loading and dynamic stall effects. Similarly, innovative concepts such as Minesto [51] exploit tethered underwater-kite configurations to increase relative flow velocity and enable operation in lower-current environments.

Table 1 summarises representative tidal-energy concepts together with their deployment characteristics and their relevance to long-term biofouling assessment based on the operational evidence currently available. Although tidal-energy technologies have reached an increasing level of maturity, the amount of field evidence directly linking biofouling to turbine performance remains limited. Most published studies are still based on laboratory-scale experiments, numerical simulations, short-term deployment campaigns, or retrieval inspections, whereas

**Table 1**
Representative marine current turbine concepts and their relevance for long-term biofouling assessment based on current operational experience.

| Technology | Configuration | Deployment | Operational evidence and biofouling relevance |
|---|---|---|---|
| MeyGen [32] | HATT | Gravity-based | Long-term commercial operation under energetic tidal conditions; operational experience is available, but quantitative evidence relating biofouling to power-performance degradation remains limited |
| SeaGen [33,34] | HATT | Monopile | Early commercial-scale deployment demonstrating prolonged marine exposure; only limited operational evidence on biofouling-induced performance losses has been reported |
| Orbital Marine Power [38,39] | Floating HATT | Floating | Floating configuration facilitates inspection, retrieval and cleaning operations; long-term biofouling-performance data are still scarce |
| Sabella D10 [36] | HATT | Gravity-based | Commercial deep-water deployment providing operational experience under prolonged marine exposure; quantitative biofouling-performance assessments remain limited |
| Hammerfest [35] | HATT | Gravity/piles | Early offshore full-scale deployment demonstrating long-term operation; limited published evidence on biofouling effects is currently available |
| OpenHydro [42] | Ducted HATT | Gravity-based | Operational ducted concept highlighting the importance of shroud fouling; quantitative field evidence on biofouling remains limited |
| GEM/GEMSTAR [40,41] | Ducted HATT | Tethered | Tethered configuration improves accessibility for maintenance; further long-term field evidence is required to quantify biofouling effects |
| HydroQuest [48,49] | VATT | Gravity-based | Operational vertical-axis concept potentially affected by roughness-induced degradation; field evidence remains limited |
| Kobold [3,44,45] | VATT | Floating | Floating prototype enabling straightforward maintenance operations; operational biofouling studies are still scarce |
| Gorlov [46,47] | Helical VATT | Bottom-mounted | Helical blades mitigate cyclic loading; limited operational evidence is available regarding long-term biofouling effects |
| Minesto [51] | Tethered turbine | Floating/Tethered | Variable immersion depth may influence fouling development; operational evidence on biofouling-induced performance degradation is currently limited |

quantitative observations from long-term commercial operation remain scarce. Consequently, the interaction between turbine architecture, deployment strategy, biofouling evolution, and long-term performance degradation is still only partially understood, particularly under realistic offshore operating conditions.

## 3. Effects of long term deployment

### 3.1. Integrated framework of long-term biofouling impacts

The long-term deployment of marine current turbines involves the interaction of hydrodynamic, environmental, biological, and operational processes acting simultaneously on the energy conversion system. Unlike conventional short-term hydrodynamic analyses, long-term operation in marine environments progressively exposes turbine blades, support structures, mooring systems, and submerged components to marine growth, corrosion, and surface degradation phenomena. Among these mechanisms, biofouling is one of the most critical challenges because it directly modifies surface roughness and flow behaviour, while also affecting inspection procedures, maintenance requirements, and operational reliability. The development of marine growth depends strongly on local environmental conditions such as current velocity, turbulence intensity, temperature, salinity, nutrient availability, biological productivity, and installation depth. Consequently, different turbine configurations and deployment strategies may experience significantly different fouling conditions during operation. Bottom-mounted systems operating in highly energetic sites may partially benefit from elevated wall shear stress, which can limit marine growth on some rotating surfaces, whereas floating and tethered systems generally introduce additional submerged components exposed to long-term fouling accumulation. Similarly, ducted or shrouded turbines may experience performance degradation not only due to increased blade roughness, but also because of fouling accumulation on internal duct surfaces, which affects flow acceleration and pressure recovery. Biofouling-induced degradation therefore cannot be interpreted solely as a local surface roughness issue. The effects propagate across multiple scales, from blade hydrodynamics and wake development to maintenance strategy, energy production, and overall techno-economic performance. Surface roughness modifies lift and drag coefficients, alters boundary-layer behaviour, and may shift the optimal tip-speed ratio of the turbine. Simultaneously, marine growth increases inspection and cleaning requirements, contributes to maintenance downtime, and may accelerate coating degradation and structural loading.

Fig. 1 summarises the coupled mechanisms linking environmental forcing, marine growth development, hydrodynamic degradation, and the resulting operational and techno-economic impacts on marine current turbines.

The framework highlights the progressive chain linking environmental exposure, fouling growth, surface degradation, hydrodynamic performance losses, maintenance requirements, and lifecycle economic penalties. This integrated perspective is particularly important because most current studies still investigate isolated aspects of biofouling, while coupled analyses that include hydrodynamic, operational, and economic effects remain relatively limited in the existing literature.

### 3.2. Biofouling on MCTs

Marine energy devices operate in harsh environments that demand high reliability and durability. Biofouling is a major challenge in the marine environment, as it affects moorings, as well as floating and submerged components of energy converters, and influences the longevity, durability, and performance of energy conversion. As illustrated in Fig. 2, biofouling involves the attachment and growth of various communities of organisms on surfaces immersed in seawater. It can be categorised, according to body size, into two types: microfouling and macrofouling [52–54].

Microfouling (also known as biofilms) is generally the initial stage of biofouling development, in which bacteria and other microorganisms begin to colonise the immersed surface. Macrofouling is the colonisation by larger organisms, which can be divided into hard fouling and soft fouling. The latter have soft bodies, such as macroalgae, tunicates, and hydroids. Hard fouling, on the other hand, consists of organisms with a rigid outer layer, usually made of calcium carbonate, including barnacles, calcareous tubeworms, oysters, and mussels [56].

The growth of biofouling on turbine blades is influenced by several environmental and geographical factors, such as local current speed and turbulence, water quality, salinity and seawater pH [53], seawater temperature [57–59], water depth, light availability, seafloor topography, distance to shore [60], the material of the turbine blades, the choice of coating, and deployment duration [61,62]. Fig. 3 illustrates the development of biofouling on four marine current turbines over different deployment periods.

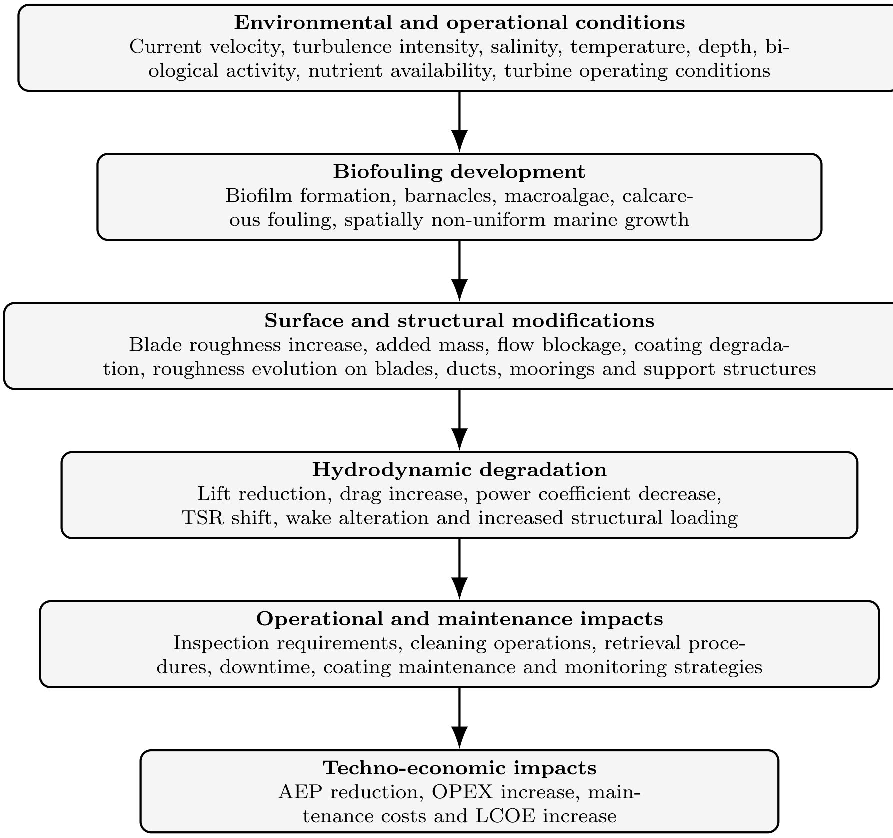


**Fig. 1.** Integrated framework describing the effects of biofouling on marine current turbines, from environmental forcing and marine growth development to hydrodynamic, operational and techno-economic impacts.

**Fig. 2.** Biofouling community observed on the foundation of a gravity-based offshore wind turbine in Belgium, including blue mussels, plumose anemones, sea urchins, common starfish, barnacles, and tubeworms [55].

### 3.3. Performance degradation

Biofouling-induced performance degradation should not be modelled as a single time-dependent loss factor, as both the hydrodynamic penalty and the biological growth rate depend strongly on turbine topology, installation depth, and site-specific sea conditions. A more general modelling framework should therefore distinguish between: (i) the biological fouling state, described by thickness, coverage, and morphology; (ii) the hydrodynamic response of the turbine; and (iii) the operational strategy, including TSR control and maintenance intervals.

For bottom-mounted horizontal-axis tidal turbines (HATTs), the dominant modelling approach is based on RANS or BEM simulations coupled with roughness wall functions or degraded airfoil polars. These approaches show that biofouling reduces the power coefficient and shifts the optimal TSR towards lower values.

For vertical-axis tidal turbines (VATTs), the effect of fouling interacts with dynamic stall and cyclic loading, requiring unsteady models (URANS/LES or streamtube-based approaches with corrected polars). Therefore, results obtained for HATTs are not directly transferable to VATT configurations.

In ducted or shrouded turbines, fouling on both the rotor and duct must be considered, as roughness on the inner duct surface can reduce flow acceleration and pressure recovery, resulting in additional performance losses beyond those caused by blade roughness alone.

Installation depth and environmental conditions also influence fouling type and growth rate. Near-surface deployments are more exposed to macroalgae and light-driven organisms, while deeper installations are typically dominated by biofilm and calcareous fouling. Therefore, biofouling models should include both growth and detachment mechanisms, depending on local flow velocity and shear stress.

Table 2 summarises the main biofouling-related degradation mechanisms associated with different tidal turbine typologies, together with the corresponding modelling approaches commonly adopted in the literature.

### 3.4. CFD-based modelling of biofouling-induced performance degradation

Computational Fluid Dynamics (CFD) is currently the most comprehensive numerical tool for quantifying the hydrodynamic effects of biofouling on marine current turbines. Unlike empirical or Blade Element Momentum (BEM) approaches, CFD can resolve local flow modifications caused by blade roughness, biofilms, barnacles, duct fouling, and support-structure colonisation, providing predictions of the power coefficient ($C_P$), thrust coefficient ($C_T$), torque, wall shear stress, wake

(a) Fouled condition of the SCHOTTEL Instream Turbine (SIT), achieved by keeping the rotor in the water without operating it for approximately four weeks (63).

(b) Fouling after six months of the NOVA Innovation turbine (64) (Clean Current Tidal Power Demonstration Project).

(c) The HydroQuest tidal turbine was retrieved in late September 2021 after two years submerged and operating at the Paimpol-Bréhat site. (65).

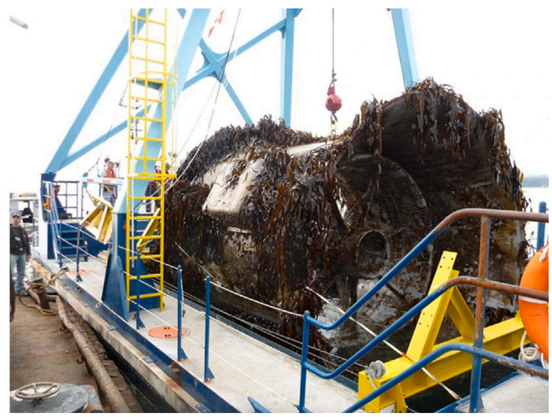

(d) Ducted axial-flow tidal current turbine after three years of deployment in the Race Rocks Ecological Reserve in British Columbia, Canada (66).

**Fig. 3.** Examples of biofouling observed on marine current turbines after various deployment periods at different installation sites [63–66].

**Table 2**
Biofouling impact and modelling approaches for different tidal turbine types.

| Turbine type | Installation/environment | Main fouling effects | Recommended modelling approach |
|---|---|---|---|
| Bottom-mounted HATT | Mid/deep water, high currents, turbulent flow | Blade roughness, reduced lift-to-drag ratio, shift of optimal TSR | RANS/BEM with roughness wall functions; degraded airfoil polars |
| Floating HATT | Near-surface, wave-current interaction, high biological activity | Fouling on blades, hull and moorings; variable inflow conditions | Coupled hydrodynamic-platform models with roughness effects |
| Vertical axis turbines (VATT) | Reversing flows, cyclic loading | Fouling affects dynamic stall, torque ripple and fatigue | URANS/LES or streamtube models with fouled blade polars |
| Ducted/shrouded turbines | Confined flow, internal surfaces exposed | Fouling on duct reduces flow acceleration and pressure recovery | CFD with roughness on rotor and duct; possible explicit macrofouling |
| Tethered/kite systems | Variable depth, trajectory-dependent flow | Non-uniform fouling; possible self-cleaning due to motion | Time-dependent growth-detachment models coupled with trajectory |
| Tidal farms/arrays | Wake interaction, spatial variability | Fouling alters wake recovery and farm efficiency | Actuator disk/farm-scale models with time-dependent performance |

development, and the shift in the optimal tip-speed ratio (TSR). These quantities are essential for evaluating the impact of biofouling on Annual Energy Production (AEP) and Levelised Cost of Energy (LCOE).

Existing CFD approaches can be grouped into three main categories (see Table 3). RANS/URANS models with equivalent roughness wall functions are the most widely adopted solution because they provide a good compromise between computational cost and accuracy. Explicit macrofouling models offer higher fidelity at significantly higher computational cost, whereas CFD-informed BEM or actuator-based models are particularly suitable for long-term simulations and farm-scale analyses.

A reliable CFD workflow should include the definition of the fouling state, its representation through equivalent roughness or explicit geometry, mesh generation, selection of the numerical model, computation of the main hydrodynamic quantities ($C_P$, $C_T$, torque and wake characteristics), and validation against experimental or field data. Without proper validation, predictions may be significantly affected by numerical uncertainty, wall-function assumptions, and turbulence-model sensitivity.

The main limitation of current CFD-based approaches is that they generally predict the performance penalty for a prescribed fouling

**Table 3**
CFD approaches for predicting biofouling-induced performance degradation in marine current turbines.

| CFD approach | Fouling representation | Main application | Main limitation |
|---|---|---|---|
| RANS/URANS with rough-wall functions | Equivalent sand-grain roughness $k_s$ and roughness constant $C_s$ | Biofilm, distributed roughness, parametric TSR studies | Requires calibration of equivalent roughness and valid wall-function range |
| Full-rotor CFD with MRF | Prescribed roughness on blades, hub or duct | Fast prediction of $C_P$–TSR and $C_T$–TSR curves | Quasi-steady approximation; limited unsteady wake information |
| Full-rotor CFD with sliding mesh | Time-dependent blade motion with fouled surfaces | Unsteady loads, wake interaction, non-uniform fouling | Higher computational cost than MRF |
| Explicit macro-roughness CFD | Barnacles or protrusions modelled as real geometry | Local separation, leading-edge fouling, duct lip fouling | Very fine mesh required; difficult for full-scale lifetime studies |
| LES/hybrid RANS–LES | Resolved roughness or high-fidelity rough-wall treatment | Vortex dynamics, wake recovery, dynamic stall | Computationally expensive; mainly suited to reference cases |
| BEM/actuator models informed by CFD | Fouled airfoil polars or roughness-corrected sectional data | AEP, arrays, long-term scenario analysis | Accuracy depends on the quality of the fouled polar database |

**Table 4**
Effects of biofouling on ships, propellers and submarines.

| Study | Method | Biofouling type | Main results |
|---|---|---|---|
| Farkas et al. [69] | CFD open-water prediction with roughness models on three marine propeller geometries | Blade surface roughness (roughness functions in CFD) | Thrust, torque and efficiency strongly sensitive to blade roughness; rapid workflow for performance forecasting and maintenance planning |
| Coraddu et al. [73] | Data analysis measured by on-board systems on the Research Vessel (*The Princess Royal*), unsupervised by Machine Learning | Real fouling condition | Novelty detection separates hull fouling from machinery effects without labels; supports timely cleaning |
| Uzun et al. [74] | RANS CFD with wall-roughness functions on full-scale submarine (self-propulsion) | Barnacle-type roughness (homogeneous vs heterogeneous distribution) | Roughness increased resistance and delivered power; forward-hull fouling produced largest penalties; partial fouling non-negligible |
| Song et al. [75] | URANS with Proportional Integral controller on container ship (full-scale self-propulsion) | Barnacle fouling on hull, rudder, propeller (varied size and coverage) | Frictional resistance increased up to 93%, total resistance up to 73%; thrust decreased, torque increased, efficiency decreased |
| Farkas et al. [76] | Performance Prediction Method vs CFD model on Handymax bulk carrier (Halifax-Rotterdam) | Soft fouling (scenarios R1–R8) | Potential savings: $38,000 fuel and 327 t $CO_2$ per voyage with optimal cleaning; soft fouling penalties are often underestimated |
| Uzun et al. [77] | RANS CFD with scale effects (Granville comparison) on full-scale submarine | Biofouling roughness grades (height-dependent functions) | Effective power increased by 36–112%; stern wake fraction increased by 25–68% |
| Demirel et al. [67] | Towing tests with artificial barnacles on flat plates extrapolated to ships | Barnacle fouling (height and coverage sweeps) | 10% coverage with 5 mm barnacles is approximately equivalent to 50% coverage with 1.25 mm barnacles in added power |
| Song et al. [71] | CFD with wall-roughness functions on full-scale propeller (open-water) | Barnacle fouling on blades (increasing severity) | Increasing barnacle fouling reduces thrust, increases torque, and decreases open-water efficiency by up to 19.3%, while also altering pressure and velocity fields |

condition, rather than predicting biological growth itself. Therefore, CFD should be integrated with site-specific biofouling observations and growth-detachment models. In such a framework, settlement-panel data provide fouling thickness, coverage, and morphology; ecological models estimate the time evolution of fouling; and CFD translates these surface conditions into hydrodynamic penalties. This integration is necessary to move from isolated performance simulations to predictive lifetime assessments of marine current turbines.

Therefore, CFD models are essential for quantifying the hydrodynamic penalty of a given fouling state, but they must be coupled with site-specific biological monitoring and growth-detachment models to become truly predictive over the turbine's lifetime.

In tidal turbines, marine growth on both fixed and moving parts can affect the performance and efficiency of the energy conversion system. Research on its effects on tidal turbines remains limited. While the impact of biofouling on the performance of ship propellers (for example, through CFD models that take into account different roughness types) has been extensively analysed to reduce fuel consumption, determine adequate cleaning intervals, and develop special coatings to extend device lifespan [67–70]. The study reported by Ref. [69] investigates the effects of two types of biofouling (biofilm and hard fouling) on the performance of three different ship propellers in open water using a CFD model validated against experimental data. The results show that biofouling reduces the pressure difference between the pressure and suction sides of the propeller blades, causing the lift coefficient ($C_L$) and thrust coefficient ($K_T$) to decrease, while wall shear stress increases, leading to an increase in the drag coefficient ($C_D$) and torque coefficient ($K_Q$). The study highlights the importance of regular propeller cleaning. To predict the fuel consumption of ships while considering the impact of biofouling on propulsion performance, Refs. [71,72] developed a CFD model that incorporates roughness wall functions to analyse different fouling scenarios and surface conditions (referred to as fouling severities). The results show that as fouling increases, the thrust coefficient decreases, while the torque coefficient increases, resulting in a decrease in the open water efficiency of the propeller.

The challenges of predicting hull and propeller fouling during real operations were investigated by Ref. [73]. The study found that the time interval for cleaning the submerged part of the ship (hull or propeller) depends on several factors, such as the type of paint covering the underwater surface, the ratio between stationary and operational periods, water temperature, and surrounding environmental conditions. Table 4 presents a comparative summary of biofouling detection on submerged parts of ships and its impact on propulsion performance.

Due to the correlation between marine growth and the duration of installation in seawater, as well as the ratio between the standing and movement times of the turbine, Ref. [78] studied an optimisation procedure for blade design to reduce turbine idle times. The authors aim to investigate the long-term biofouling effects on both moving and static parts of the GEMSTAR device [40,41], which is suited for installation in the Mediterranean Sea, under tidal current speeds that are half (see Ref. [79]) of those present in the experimental area used by Ref. [80].

The influence of blade roughness and biofouling on the performance of a two-bladed HATT was investigated both experimentally and numerically by Ref. [81]. They tested three cases: clean blades, artificially

**Table 5**
Comparative evidence from laboratory, numerical and field studies on the impact of biofouling on marine current turbine performance.

| Study | Method | Biofouling type | Main results |
|---|---|---|---|
| Walker et al. [81] | Experiments and BEM on HATT with 0.8 m rotor (1:25 scale) | Artificial roughness (sandpaper, fouling layers; leading edge versus full chord) | $C_P$ reduced from 0.42 to 0.34 (−19%); stall delayed in some cases; artificial fouling often sheared off |
| Walker et al. [83] | Experiments (unsteady flow, dynamic stall) on a blade section | Barnacle-shaped excrescences (localised roughness on suction surface) | Lift mostly unaffected; drag strongly increased; section efficiency loss up to 50–70% |
| Song et al. [64,72] | CFD (RANS with roughness wall functions) on full-scale HATT (NOVA Innovation) | Barnacle fouling ($k/c$ up to 0.006; varying coverage/height) | $C_P$ decreased up to 13%; thrust reduced; narrower efficient TSR range; optimum TSR shifted lower; efficiency loss more severe at high TSR; TSR adjustment can mitigate |
| Farkas et al. [85] | CFD with biofilm wall functions (validated) on full-scale marine current turbine | Biofilm (partial to 100% coverage, thickness scaling) | At optimal TSR: $C_P$ reduced by 10.7%; thrust also reduced; losses increase with film thickness and coverage |
| Priegue and Stoesser [82] | Flume experiments on Vertical Axis Tidal Turbine | Surface roughness (three levels) | Smooth blades $C_P$ 27–36% higher than rough; roughness only beneficial at very low Reynolds number; at relevant chord Reynolds number, the turbine with the highest solidity rotor performed best |
| Starzmann et al. [63] | Field tests and BEM on SIT platform (PLAT-I, four rotors of 6.3 m) | Natural fouling (biofilm and macroalgae, $k/c \sim 0.006$–$0.03$) | Power decreased by 43–47%; thrust decreased by 22–28% |
| Afshar [84] | CFD (RANS SST) and flat-plate drag tests | Barnacle roughness (low, medium, high density) | Lift reduced by 21%; $L/D$ ratio reduced by 60%; $C_P$ dropped from 0.42 (clean) to 0.37 (fouled); long-term power decrease up to 22% |
| Rashid et al. [87] | Neural network models trained on datasets from the Tidal Stream Turbine platform at Shanghai Maritime University (SMU) and the tidal turbulence test facility at Lehigh University (LU) | Biofouling detection via ML (images classified as clean, light, heavy) | Detection accuracy: 83% (SMU) and 90% (LU); larger datasets improved robustness |

fouled blades, and roughened blades. While tests on artificially fouled blades showed no performance degradation, as most of the fouling came off, the roughened blades showed a performance degradation of up to 19% compared to the clean blades. These results were confirmed numerically. Similar results were found by Refs. [64,75], which investigated numerically the effects of roughness induced by biofouling on the performance of a horizontal-axis tidal turbine. The authors conducted several CFD simulations based on the Reynolds-Averaged Navier-Stokes (RANS) equations for different fouling scenarios and tip speed ratios (TSR), using a wall function to simulate surface roughness. The results revealed that the power coefficient ($C_P$) decreases as biofouling increases, with the greatest losses occurring at higher TSRs. Specifically, the maximum value of $C_P$ occurs at lower TSRs as surface roughness increases, indicating that a fouled turbine operates most efficiently at a lower speed than a clean turbine.

Contrary to the findings of [81], which reported that artificially fouled material improved performance by delaying stall to higher angles of attack, the tests conducted by Ref. [82] did not confirm any benefit in terms of delay or reduction of dynamic stall. They highlighted the negative effect of increased blade roughness, which becomes more pronounced as the blade Reynolds number increases. Furthermore, they examined the combined effects of blade roughness and rotor solidity, demonstrating that rotor solidity and the number of blades have a similar impact on performance as blade roughness. The performance of marine current turbines, as with wind turbines, is highly sensitive to the lift and drag coefficients. The effect of biofouling on blade performance, specifically when barnacles grow on the suction side of the blade section, was investigated by Ref. [83]. It was found that the hydrodynamic power coefficients change due to the presence of a barnacle, with an increase in the drag coefficient, while no significant effect on the lift coefficient was observed. Similar results for the drag coefficient, along with a reduction in the lift coefficient, have been found numerically by Ref. [84], who considered adult barnacle roughness on a NACA63-618 aerofoil. The most recent Scopus article on the problems caused by biofouling in marine current turbines (MCTs) to date is [85]. This study modelled full-scale CFD simulations considering six fouling conditions by varying biofilm height and percentage of surface coverage at different tip speed ratios (TSRs), using a wall function described by the authors in [86]. The simulations were validated by comparing the results with experimental and numerical data from the literature [81]. The study found a decrease in both power and thrust coefficients, and that the trend of decrease in the power coefficient does not follow the increase in the roughness length scale of the biofilm. As previously described by several studies, the maximum of the power coefficient curve shifts towards lower TSR.

Table 5 compares the principal experimental, numerical, and field investigations available in the literature. Although laboratory experiments and CFD simulations still dominate current research, the limited evidence obtained from full-scale deployments and operational tidal turbines confirms that natural biofouling can produce substantially larger performance penalties than those generally observed under controlled conditions. These field observations therefore play a key role in validating predictive models and assessing the long-term impact of biofouling on power generation.

Overall, the comparison highlights a progressive evolution of the literature from controlled laboratory investigations towards full-scale numerical simulations and operational field observations. However, despite these recent advances, long-term datasets collected on commercial tidal turbines remain limited, reinforcing the need for extended monitoring campaigns under realistic operating conditions.

### 3.5. Maintenance and mitigation strategy

Biofouling mitigation in marine current turbines requires an integrated combination of surface treatments, operational control, and scheduled maintenance. The effectiveness of each strategy depends on the turbine component, local hydrodynamic conditions, fouling type, required durability, environmental constraints, and maintenance accessibility.

Antifouling coatings can be broadly divided into biocide-based systems, including self-polishing copolymers (SPCs), and non-toxic foul-release coatings. SPC coatings progressively erode and release antifouling agents, but their environmental impact and durability under high-speed marine flows remain significant limitations. Foul-release coatings, generally based on silicone or fluoropolymer matrices, instead reduce organism adhesion and may promote partial self-cleaning on rotating blades through hydrodynamic shear.

Emerging solutions include hydrophilic and zwitterionic materials, biomimetic micro-textured surfaces, and slippery liquid-infused porous surfaces (SLIPS), which aim to limit early biofilm formation by modifying surface energy, wettability, or interfacial interactions. However, their full-scale application remains constrained by abrasion resistance,

**Table 6**
Comparison of the main biofouling mitigation strategies proposed for marine current turbines.

| Mitigation strategy | Typical application | Main advantage | Main limitation |
|---|---|---|---|
| Self-polishing copolymer (SPC) coatings | Blades, ducts, support structures | Long-term antifouling protection | Environmental concerns; progressive coating consumption |
| Foul-release coatings | Rotor blades and rotating components | Low organism adhesion and partial self-cleaning under hydrodynamic loading | Limited durability under severe operating conditions |
| Adaptive TSR control | Rotor operation | Partially compensates biofouling-induced performance losses | Does not prevent fouling development |
| Mechanical cleaning | Rotor, ducts, support structures | Immediate recovery of hydrodynamic performance | Operational downtime and maintenance costs |
| Component-specific maintenance | Entire turbine | Optimises inspection and maintenance scheduling | Requires continuous monitoring and site-specific planning |
| Combined antifouling and anticorrosion systems | Foundations and submerged structures | Simultaneous protection against fouling and corrosion | Long-term coating degradation and maintenance requirements |

mechanical durability, long-term stability, and cost under realistic offshore conditions.

Operational strategies provide a complementary means of reducing performance losses. Low-speed rotation during non-generating periods may limit settlement, while adaptive tip-speed-ratio (TSR) control can partially compensate for the shift in optimal operating conditions caused by surface roughness. Nevertheless, these approaches mitigate the consequences of fouling rather than preventing its development.

Finally, mitigation strategies should be tailored to the specific turbine component and operating conditions. Since no single solution is universally effective, coating technologies, operational control, and maintenance scheduling should be regarded as complementary rather than alternative approaches. Their relative advantages and limitations are summarised in Table 6.

The comparison reported in Table 6 shows that the available mitigation strategies address different aspects of biofouling and should therefore be combined to maximise long-term turbine performance. Recent studies have consequently investigated both operational solutions and advanced coating technologies, together with optimised maintenance planning, to reduce hydrodynamic penalties while limiting maintenance costs.

Considering this phenomenon in the design process of a hydrofoil to improve performance during operation is a maintenance strategy suggested by Ref. [85]. Specifically, as a consequence of the results described in the previous Section, according to [64,75], an important practical implication can be highlighted: adjusting the turbine's TSR based on the level of biofouling could be an effective strategy to maintain high efficiency and maximise energy production. Antifouling paints can be used to prevent biofouling. Tributyltin (TBT) is among the most effective antifouling agents and has been used in the past, despite its undesired effects on non-target marine organisms [88]. As an alternative to these chemical methods, silicon-based, low surface energy coating materials are used, known as "Foul Release" technology [89]. After its commercialisation, Ref. [90] measured the drag coefficient and roughness characteristics of variously sized flat plates coated with polydimethyl-siloxane (PDMS) foul-release and tin-free copper-pigmented acrylic Self-Polishing Copolymers (SPC) coatings in a towing tank, comparing the results. Similar experiments were conducted on uncoated and coated cylinders to assess differences in torque. Assuming that the increase in drag caused by marine growth on the blades is similar to that observed for slow-moving vessels, Ref. [52] simulated the power losses of a full-scale 1 MW marine turbine after five years of exposure, considering different coating systems. It was assumed that tidal currents are present for an average of 12 hours per day and that the turbine operates at 90% of its rated power during this period. The study found that the energy loss from a single turbine, when extrapolated to a hypothetical 600 MW farm, amounts to 3.69 GWh in the worst-case coating scenario.

The authors also examined the decline in turbine performance by comparing two types of antifouling products. They found that fouling release paints are more efficient in the first 1–2 years but tend to accumulate fouling more rapidly than the best biocide-based products. However, over their lifetime, these coatings tend to self-clean periodically (see Fig. 4 of [52]).

CFD simulations were employed by Ref. [91] to analyse the effects of biofouling and antifouling treatments on the hydrodynamic performance of the NACA 4424 airfoil and the Defence Research Establishment Atlantic (DREA) submarine hull. They investigated different levels of fouling by placing small conical shapes on the surface of the airfoil and examined two antifouling strategies to mitigate these negative effects (SPC and Foul-Release Coatings), using the roughness characteristics previously examined by Refs. [90,92]. For the NACA 4424 airfoil, fouling reduces the lift-drag ratio by up to 80%, resulting in a significant increase in fuel consumption. Results obtained with Foul-Release Coatings are very close to those obtained in the case of no fouling, significantly improving hydrodynamic efficiency compared to SPCs. This is because SPC generates higher turbulence near the boundary layer, reducing the $C_L/C_D$ ratio compared to Foul-Release Coatings. Although the cost of applying SPC to ship hulls is lower, the increased drag can negate this benefit, making Foul-Release Coatings the more cost-effective choice.

The effects of the coatings and antifouling technologies are summarised in Table 7.

Table 8 presents a summary of biofouling effects on tidal turbines. As shown, biofouling typically reduces tidal turbine performance by 10–20% under moderate fouling, while severe natural colonisation can cause up to 45% power loss. The impact depends strongly on the type of fouling (biofilm, barnacle, or macroalgae), but in all cases, efficiency losses are rapid and nonlinear. Without proactive antifouling measures and monitoring, long-term energy yield is severely compromised.

To quantify the performance degradation of tidal turbines after long-term deployment in the marine environment, the relationship between the type of biofouling, its characteristic dimensions, and the corresponding power losses reported in the literature was examined. Several studies in marine biology classify fouling organisms based on their typical size (e.g., from biofilms to macrofouling layers such as barnacles, tubeworms, and macroalgae) [58–60].

Through this association, it was possible to compare the effect of fouling morphology on hydrodynamic performance. Fig. 4 summarises the efficiency losses reported in various studies as a function of fouling thickness, $\delta$, and fouling type. It should be noted that the relationship between fouling type and its characteristic size (in mm) was not always explicitly reported in the reviewed studies. Therefore, in this work, the association between each data point and the corresponding fouling type (or characteristic size) was made according to typical quantifications of the considered biofouling categories, as derived from marine biology and antifouling literature [58–60,95,96]. The reduction in the power coefficient is defined as

$$\Delta C_p = \frac{C_{Ps} - C_{Pf}}{C_{Ps}}, \quad (1)$$

**Table 7**
Summary of coatings and antifouling technologies.

| Study | Method | Biofouling/coating type | Main results |
|---|---|---|---|
| Khor and Xiao [91] | CFD simulations (varied roughness height) on an aerofoil and submerged hull | Barnacles; Self-Polishing Copolymer (SPC) vs foul-release coatings | $CL/CD$ decreased by up to 80 Korkut and Atlar [89] |
| Experiments (model scale on marine propeller, full coverage) | Foul-release coating | No efficiency loss; cavitation slightly reduced; lower noise in non-cavitating conditions. | |
| Hunsucker et al. [56] | Experimental approach on panels with five commercial coatings after four months' immersion | Mixed biofilm and calcareous fouling (high vs low profile organisms) | Biofilm increased power by 16–21%; calcareous fouling increased power by 59–86%; coating type influences removal |
| Löschau and Krätke [88] | Experimental approach on Self-polishing antifouling paints; bioassays with barnacle larvae and algae | Biocide-free SPC paints | Effective against barnacle settlement but toxic effects observed; Zn release and solvents contributed to toxicity |
| Yebra et al. [53] | Review of antifouling paints | Historical SPC, tin-free biocides, foul-release coatings | Without coatings: fuel increase up to 40%, voyage costs up to 77% |
| Candries et al. [92] | Drag tests at different Reynolds numbers | SPC vs foul-release coatings (tin-free, full coverage) | Foul-release coatings consistently showed lower drag than SPC; confirmed smoother surface and reduced resistance |
| Yebra et al. [52] | Conceptual assessment | Generic fouling (biofilm and macrofouling) and coating options | Estimated significant efficiency loss of tidal turbines due to fouling; highlighted offshore maintenance challenges and the importance of coating selection |
| García et al. [93] | CFD (OpenFOAM RANS solver validated with experimental roughness data) | Four different commercial fouling control coatings were used: a hydrolysing silyl acrylate self-polishing copolymer (SA-SPC), an ablative copper-based system (Cu-Abl), a copper acrylate self-polishing copolymer | CFD predicted a total drag increase of up to 136% for heavy fouling and approximately 10–30% power rise depending on coating type |
| Tang et al. [94] | Laboratory tests on steel samples (electrochemical impedance, adhesion) | Innovative RF/epoxy composite coating (full coverage) | Corrosion resistance about 100 times higher than pure epoxy; strong antibacterial (*E. coli*, *S. aureus*) and anti-algal (*Chlorella*) resistance |

**Table 8**
Typical and maximum loss on tidal turbines for different types of biofouling.

| Biofouling type | Typical loss | Maximum reported loss |
|---|---|---|
| Biofilm [56,74,85,86] | ~5–10% reduction in $C_P$ | Up to 11% |
| Barnacles [64,67,71,72,74,81,83,84] | 10–20% reduction in $C_P$ | Up to 22% |
| Macroalgae [63] | ~40% power loss | Up to 47% |
| Mixed fouling (biofilm + calcareous or macrofouling) [52,53,56] | 15–20% (biofilm) to 60–80% (hard calcareous) powering increase in ship/tow tests | Up to 86% |

where $C_{P_s}$ and $C_{P_f}$ represent the power coefficients for the smoothed and fouled conditions, respectively. Each point represents an individual study, grouped by fouling type. Furthermore, the comparison shown in Fig. 4 should be interpreted qualitatively rather than as a universal predictive correlation, as the reviewed studies involve different Reynolds numbers, turbine geometries, fouling morphologies, surface coverage ratios, and operating conditions. Therefore, the observed trends mainly illustrate the general increase in hydrodynamic penalties with increasing fouling severity, rather than a unique quantitative relationship. As observed and reported by Ref. [83], biofilm or early microfouling (defined as having a thickness less than 0.5 mm) causes power-coefficient reductions approaching 10%. Small barnacle growth (with a height of 1–2 mm) and varying surface coverage (between 10% and 50%), as reported by Refs. [71,72], results in power-coefficient decreases of up to 13%. In turbines with artificial roughness and barnacle-shaped excrescences (with a thickness of around 2–3 mm), losses increase rapidly, reaching 19% for general roughness and 50–70% for localised barnacle formations [81,83].

Medium to large barnacles (about 5 mm in height) were analysed on flat plates by Refs. [63,67], and the results show power losses ranging between 43% and 47%.

Lastly, Refs. [52,53,56] have reported severe calcareous or mixed fouling (greater than 10 mm), corresponding to the highest degradation levels, with power losses ranging from 60% up to 86%. In summary, biofilm or early microfouling typically causes modest performance decreases of only a few to several tens of percent. In contrast, heavy calcareous or mixed fouling can reduce turbine efficiency by up to 70%. This trend highlights the strong sensitivity of hydrodynamic efficiency to the stage of biofouling and the nonlinear relationship between fouling thickness and turbine performance reduction.

### 3.6. Site-specific experimental assessment of biofouling risk

In addition to the hydrodynamic and techno-economic analyses discussed above, site-specific experimental investigations should be considered to characterise the local biofouling risk before deploying tidal turbines. Such investigations should not be regarded as substitutes for the engineering and environmental surveys required to assess site suitability, such as tidal resource characterisation, bathymetric and geophysical surveys, geotechnical investigations, cable route assessment, metocean characterisation, navigation constraints, and environmental impact assessment. Rather, biofouling experiments provide a complementary dataset that links local biological colonisation processes with long-term turbine performance, maintenance planning, and coating selection.

A practical approach involves deploying instrumented test frames equipped with settlement panels and representative material coupons within the candidate installation area. The panels should reproduce the main materials and coatings expected in the turbine system, including blade materials, coated steel, composite materials, antifouling coatings, and foul-release coatings. As biofouling depends strongly on depth, light availability, flow velocity, turbulence, and surface orientation, the test panels should be installed at depths representative of the rotor, hub, support structure, duct, or mooring system. Different orientations relative to the dominant tidal flow should also be considered, as settlement and growth may vary between upstream-facing, downstream-facing, and sheltered surfaces.

The experimental programme should cover at least one seasonal cycle, with intermediate retrievals after approximately 3–6 months and longer exposure periods of 12 months or more. Each retrieval should quantify biofouling coverage, biomass, wet and dry mass per unit

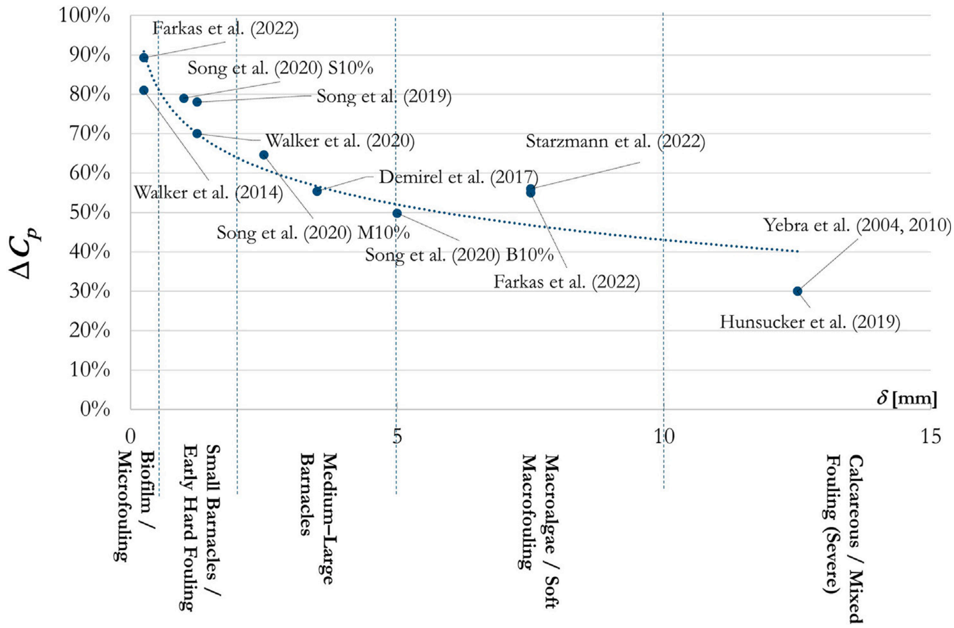


**Fig. 4.** The impact of the type of biofouling on the performance.

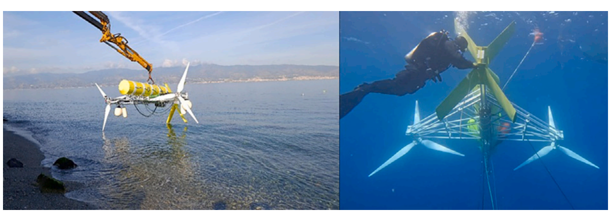

**Fig. 5.** Deployment and installation of the GEMSTAR prototype at the Renew-MEL laboratory in the Strait of Messina.

area, layer thickness, dominant taxa, macrofouling morphology, surface roughness, and adhesion strength. These biological measurements should be coupled with local environmental data, including current velocity, turbulence intensity, temperature, salinity, dissolved oxygen, pH, turbidity, chlorophyll concentration, light availability, and suspended sediment concentration. Where possible, ADCP measurements and environmental sensors should be co-located with the test frames to correlate fouling growth with the local hydrodynamic regime.

A recent example of this approach is the ongoing experimental activities associated with the GEMSTAR tidal-energy system, currently being deployed and tested in the Strait of Messina at the Renew-MEL laboratory. The experimental campaign includes hydrodynamic and structural blade design, prototype manufacturing, and open-sea deployment under realistic operating conditions. Particular attention has been given to site characterisation and anchoring-system definition, as local seabed morphology and environmental conditions strongly influence both installation strategy and long-term biofouling exposure.

The installation and deployment of the GEMSTAR prototype in the Strait of Messina are shown in Fig. 5. Although the experimental campaign is primarily focused on turbine performance characterisation, the long-term deployment of the system under real marine conditions also provides an important opportunity to investigate site-specific biofouling evolution on blades, mooring systems, and submerged structural components.

The retrieved samples can also be used to derive hydrodynamic input parameters for turbine performance models. For example, measured fouling thickness, coverage and morphology can be translated into an equivalent roughness height or used to define representative fouled airfoil geometries. These data can then be introduced into BEM, RANS or reduced-order performance models to estimate the corresponding variation in lift, drag, thrust and power coefficients. In this way, the site-specific biofouling experiment provides a direct bridge between local ecological conditions and the performance degradation models discussed in Section 3.2.

Several studies support the relevance of this approach. Want et al. [97] developed an in situ system based on settlement panels to monitor biofouling growth and test antifouling coatings at depths representative of full-scale marine renewable energy devices in energetic sites in Orkney. The BioFREE project [98], also proposed a standard monitoring system including settlement panels, data loggers, and representative materials to characterise fouling communities across marine renewable energy habitats. Moreover, Ref. [99] showed that coating type, colour, and deployment timing can influence fouling assemblages and the presence of non-native species in a marine renewable energy context. These studies demonstrate that biofouling is highly site-specific and that local experimental campaigns can inform coating choice, maintenance scheduling, and deployment timing.

For tidal turbines, this information is particularly important because biofouling affects not only biological colonisation but also hydrodynamic performance and structural loading. Heavy fouling may increase drag and added mass on support structures and moorings, while roughness on blades can reduce the lift-to-drag ratio and shift the optimal tip speed ratio. Therefore, site-specific biofouling tests should be integrated into the broader site assessment workflow. The resulting data can support three key decisions: selection of antifouling or foul-release coatings, definition of inspection and cleaning intervals, and estimation of long-term AEP and LCOE penalties due to biofouling.

### *3.7. Predictive modelling of site-specific biofouling: current limitations and proposed framework*

Although several studies have experimentally characterised biofouling communities at marine renewable energy sites, truly predictive models for tidal turbines remain limited. Existing approaches can be grouped into four main categories: site-specific monitoring studies, ecological or spatial marine growth models, hydrodynamic performance models with prescribed fouling conditions, and data-driven detection

**Table 9**
Predictive capability of existing approaches for biofouling assessment in tidal turbine applications.

| Approach | Typical output | Predictive capability | Main limitation |
|---|---|---|---|
| Settlement panels and in situ monitoring | Fouling coverage, biomass, taxa, coating performance | Experimental calibration | Does not directly predict future fouling without a growth model |
| Ecological or spatial marine growth models | Fouling thickness, biomass or fouling risk maps | Predictive at site or regional scale | Rarely coupled with turbine hydrodynamics |
| CFD or BEM performance models | $C_P$, $C_T$, torque, thrust and TSR shift | Predictive for prescribed fouling states | Require fouling thickness, coverage or roughness as input |
| Machine learning diagnostics | Fouling detection and classification | Diagnostic or monitoring capability | Usually estimates present condition rather than future growth |
| Integrated biofouling-AEP-LCOE framework | Performance, energy yield and cost penalties | Proposed research direction | Requires site-specific validation and long-term datasets |

methods. Each approach provides useful information, but none alone can fully predict the complete chain from local environmental conditions to biofouling growth, turbine performance degradation, annual energy production, and LCOE.

Site-monitoring campaigns based on settlement panels, material coupons and in situ observations provide essential information on colonisation rates, fouling morphology, biomass, dominant taxa and coating performance [97–99]. These datasets are not predictive themselves, but represent the experimental basis required to calibrate site-specific growth models.

Ecological and spatial models relate fouling development to environmental variables such as temperature, depth, chlorophyll concentration, current velocity and distance from shore [58,60,62]. Hydrodynamic approaches based on CFD, BEM and experimental testing predict the performance penalties associated with prescribed fouling conditions [63,64,75,81,85], whereas recent machine-learning methods enable automated fouling detection and monitoring for digital twin applications [87,100]. However, ecological models are rarely coupled with turbine hydrodynamics, hydrodynamic models require the fouling state as an input, and current machine-learning approaches remain primarily diagnostic rather than predictive.

This review therefore highlights a relevant research gap: a fully coupled predictive framework for tidal turbines has not yet been established. Such a framework should combine site-specific biological growth, hydrodynamic performance degradation, and techno-economic assessment. A possible formulation is to describe the fouling state as a time- and space-dependent vector:

$$R_f(\mathbf{x},t) = \left\{ h_f(\mathbf{x},t), \theta_f(\mathbf{x},t), k_s(\mathbf{x},t), m_f(\mathbf{x},t) \right\}, \tag{2}$$

where $h_f$ is the fouling thickness, $\theta_f$ is the surface coverage, $k_s$ is the equivalent sand-grain roughness and $m_f$ is the fouling mass per unit area. The spatial coordinate $\mathbf{x}$ may represent the blade surface, hub, duct, support structure, mooring line or foundation.

The temporal evolution of the fouling state can be expressed as a growth–detachment balance:

$$\frac{dR_f}{dt} = G(T, S, pH, I, z, U, TI, C_{chl}, C_{sed}) - D(\tau_w, \Omega, U), \tag{3}$$

where $G$ is the biological growth term and $D$ is the detachment or removal term. The growth term depends on environmental and biological factors such as temperature $T$, salinity $S$, pH, light availability $I$, depth $z$, current velocity $U$, turbulence intensity $TI$, chlorophyll concentration $C_{chl}$, suspended sediment concentration $C_{sed}$, seasonality, material properties, and coating characteristics. The detachment term depends on wall shear stress $\tau_w$, rotor angular velocity $\Omega$, current velocity, cleaning operations, and coating properties.

The link with turbine performance can then be established by mapping the fouling state to hydrodynamic coefficients:

$$R_f(\mathbf{x},t) \rightarrow k_s(\mathbf{x},t) \rightarrow C_L(t), C_D(t) \rightarrow C_P(t), C_T(t). \tag{4}$$

For blade-dominated degradation, this mapping can be performed using fouled airfoil polars, BEM models, or CFD simulations. For ducts, hubs, support structures, and moorings, the same fouling state can be used to estimate additional drag, blockage, added mass, and changes in structural loading. The biofouling-induced power loss can be expressed as:

$$\delta_f(t) = \frac{C_{P,clean} - C_{P,fouled}(t)}{C_{P,clean}}, \tag{5}$$

which provides the direct input for AEP and LCOE models.

Building on the integrated interactions summarised in Fig. 1, the complete predictive chain can therefore be summarised as:

$$\text{Site conditions} \rightarrow R_f(\mathbf{x},t) \rightarrow C_P(t), C_T(t) \rightarrow AEP(t) \rightarrow LCOE(t). \tag{6}$$

In this framework, site-specific monitoring therefore complements conventional engineering site investigations by providing the biological information required to calibrate the proposed predictive framework. Such an approach would support turbine design, coating selection, maintenance scheduling, digital-twin implementation and long-term techno-economic assessment (Table 9).

### 3.8. Techno-economic implications of biofouling: AEP and LCOE scenario analysis

The hydrodynamic effects of biofouling discussed in previous sections have direct implications for the long-term techno-economic performance of tidal turbines. Most available studies quantify biofouling penalties in terms of power coefficient, thrust coefficient, or blade section efficiency, but the corresponding impact on annual energy production (AEP) and levelised cost of energy (LCOE) is rarely addressed explicitly. This is an important gap, as biofouling affects both the energy yield and the operational cost of tidal energy systems.

To illustrate this coupling, a simplified scenario-based model can be introduced. The annual energy production under fouled conditions is expressed in normalized form as:

$$AEP_f(t) = AEP_0\, \eta_{age}(t) \left[1 - \delta_f(t)\right], \tag{7}$$

where $AEP_0$ is the annual energy production at deployment under clean conditions, $\eta_{age}(t)$ accounts for progressive turbine ageing unrelated to biofouling, and $\delta_f(t)$ is the relative AEP loss induced by biofouling. The ageing contribution can be modelled as follows:

$$\eta_{age}(t) = (1 - d_{age})^t, \tag{8}$$

where $d_{age}$ is the annual degradation rate. The biofouling-induced loss can be represented through an asymptotic growth law:

$$\delta_f(t) = \delta_{f,\infty} \left(1 - e^{-t/\tau_f}\right), \tag{9}$$

where $\delta_{f,\infty}$ is the maximum fouling-induced loss and $\tau_f$ is the characteristic time scale of fouling accumulation.

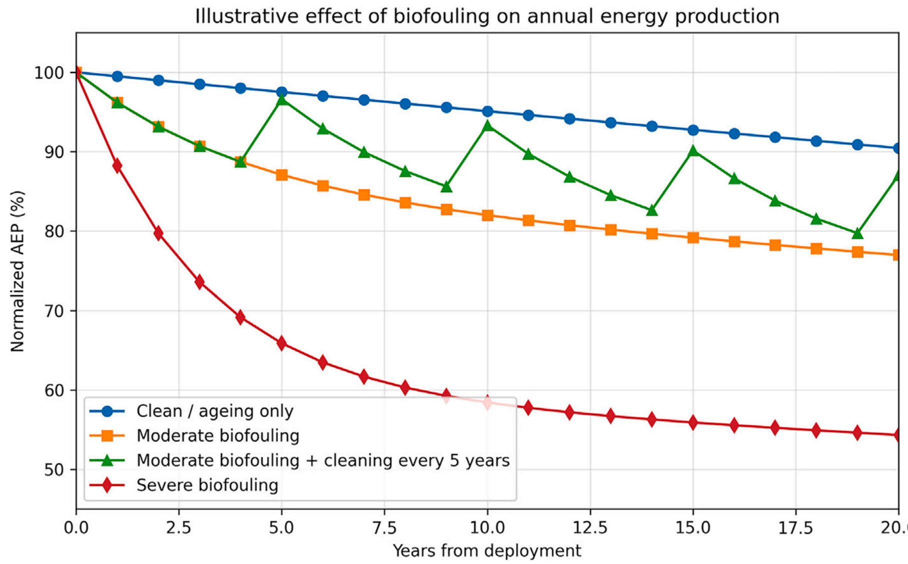


**Fig. 6.** Illustrative normalized AEP evolution over 20 years for clean operation, moderate biofouling, severe biofouling and moderate biofouling with periodic cleaning.

This formulation reflects that biofouling growth is generally rapid during the initial years after deployment and then progressively approaches a saturation level, depending on site conditions, biological activity, coating performance, hydrodynamic shear stress, and maintenance strategy. In the case of periodic cleaning, the fouling state can be partially reset at fixed maintenance intervals. If $T_c$ is the cleaning period, the exposure time since the last cleaning can be expressed as:

$$t_c = t - T_c \left\lfloor \frac{t}{T_c} \right\rfloor, \tag{10}$$

and the fouling loss after cleaning can be approximated as:

$$\delta_{f,c}(t) = \min \left[ \delta_{f,\infty}, \delta_{res}(n) + \delta_{f,\infty} \left( 1 - e^{-t_c/\tau_f} \right) \right], \tag{11}$$

where $\delta_{res}(n)$ represents the residual fouling level after the $n$th cleaning operation. This residual term accounts for incomplete removal, coating ageing, persistent biofilm, and fouling accumulation in low-shear regions such as hubs, ducts, support structures, or mooring components.

From an economic perspective, biofouling affects the LCOE through two coupled mechanisms: it reduces the annual energy production while increasing operational expenditures associated with inspections, cleaning operations, coating degradation, downtime, and possible component replacement. The LCOE was evaluated using the conventional discounted formulation widely adopted in techno-economic analyses of renewable energy systems [101,102]. Within this framework, biofouling influences the LCOE through two coupled mechanisms: it reduces the annual energy production while increasing operational expenditures associated with inspections, cleaning operations, coating degradation, downtime, and possible component replacement.

For comparative scenario analysis, the LCOE penalty can be expressed in normalized form as:

$$\Phi_{LCOE}(t) = \frac{LCOE_f(t)}{LCOE_0} = \frac{1 + \alpha_f(t)}{\eta_{age}(t)\,[1 - \delta_f(t)]}, \tag{12}$$

where $LCOE_0$ is the clean-condition reference value and $\alpha_f(t)$ is the relative increase in operational costs due to biofouling. This normalized formulation highlights the nonlinear economic impact of biofouling: reductions in AEP directly increase the LCOE, while additional maintenance and downtime costs further amplify the economic penalty.

In the illustrative scenario considered here, four cases are compared: clean operation with ageing only, moderate biofouling, severe biofouling, and moderate biofouling with cleaning every five years. The ageing rate is assumed to be $d_{age} = 0.005$ yr$^{-1}$. The moderate fouling scenario assumes $\delta_{f,\infty} = 0.15$ and $\tau_f = 4$ years, while the severe fouling scenario assumes $\delta_{f,\infty} = 0.40$ and $\tau_f = 3$ years. The corresponding asymptotic OPEX increases are assumed to be $\alpha_{f,\infty} = 0.10$ and $\alpha_{f,\infty} = 0.25$, respectively. These values are not intended as universal design parameters, but as representative ranges consistent with the performance degradation levels reported in the literature for biofilm, barnacle, macroalgal, and mixed fouling.

The results in Fig. 6 show that even moderate biofouling can significantly affect long-term energy yield. After 20 years, the clean ageing-only scenario retains about 90.5% of the initial AEP, whereas moderate biofouling reduces the normalised AEP to about 77%. Under severe fouling, the AEP decreases to approximately 54%, indicating that strong macrofouling or mixed fouling can compromise the economic viability of long-term deployment. Periodic cleaning partially restores the energy yield, increasing the normalised AEP to about 87% at year 20 in the scenario considered.

The impact on LCOE is even more pronounced. As shown in Fig. 7, the clean ageing-only case, the normalised LCOE increases to about 110% after 20 years. Moderate biofouling increases the normalised LCOE to approximately 143%, while severe fouling can increase it to about 230%. The cleaning scenario limits the LCOE increase to about 133% at year 20, despite including cleaning-related costs. This confirms that maintenance interventions can be economically justified when the recovery in AEP compensates for inspection, cleaning and downtime costs.

Overall, this simplified analysis demonstrates that biofouling mitigation should not be evaluated only in terms of hydrodynamic performance. Instead, it should be assessed through an integrated AEP-OPEX-LCOE framework, where turbine design, coating selection, monitoring strategy and maintenance planning are optimised together.

## 4. Research gaps and future directions

Despite growing interest in tidal energy technologies, knowledge of the long-term effects of biofouling on marine current turbines remains fragmented. Research agendas developed specifically for the marine renewable energy sector have identified the scarcity of site-specific biological data and operational evidence as major barriers to reliable device design and maintenance planning [103]. More recent assessments of offshore renewable energy structures similarly emphasise the limited availability of in situ offshore measurements and the incomplete

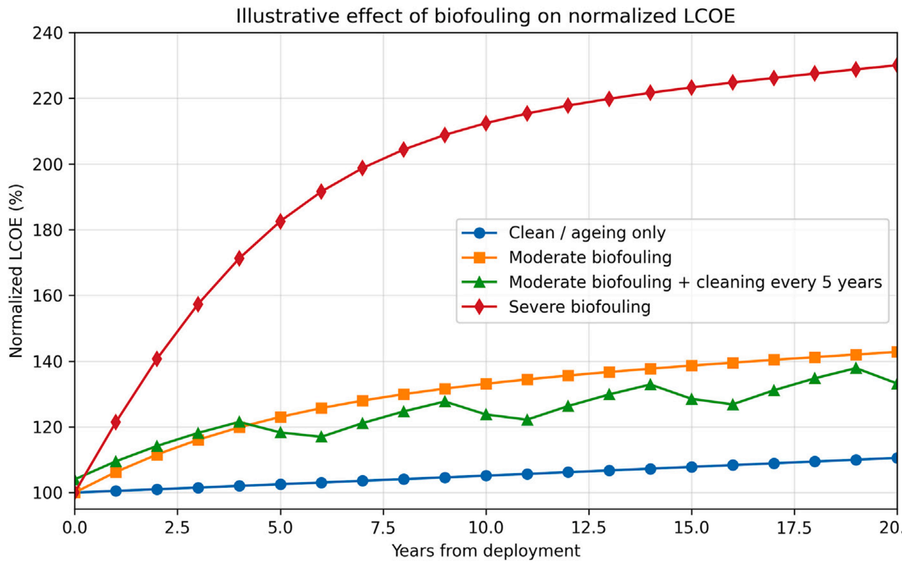


**Fig. 7.** Illustrative normalized LCOE penalty associated with biofouling-induced AEP reduction and additional OPEX.

**Table 10**
Comparative synthesis of the current literature on biofouling in marine current turbines.

| Research area | Maturity | Typical methodology | Research findings | Research gap/Future priority |
|---|---|---|---|---|
| Blade roughness and $C_P$ loss | Medium | CFD, BEM, flume tests | Power losses increase with fouling severity | Few full-scale validation datasets → Long-term validation on commercial turbines |
| Natural fouling on operating turbines | Low–Medium | Field inspections, retrieval campaigns | Natural colonisation causes significant performance degradation | Limited long-term offshore monitoring → Continuous in situ monitoring campaigns |
| Coatings for tidal turbines | Low | Laboratory tests, naval experience | SPC and foul-release coatings reduce fouling, but durability remains uncertain | Few turbine-specific durability studies → Long-term offshore qualification under tidal operating conditions |
| Biofouling growth prediction | Low | Settlement panels, ecological models | Site-specific growth can be estimated from environmental variables | Not coupled with turbine hydrodynamics → Integrated biofouling–hydrodynamic growth models |
| CFD-based degradation modelling | Medium | RANS/URANS, BEM | Hydrodynamic penalties can be predicted for prescribed fouling states | Limited validation under realistic fouling conditions → Validation using long-term full-scale datasets |
| AEP and LCOE impact | Very low | Scenario analyses | Biofouling reduces AEP and increases LCOE | No validated integrated lifecycle models → Coupled AEP–LCOE predictive frameworks |
| Farm-scale biofouling effects | Very low | Wake and array modelling | Wake effects are known only for clean turbines | No fouling–wake–farm studies → Farm-scale biofouling and array optimisation studies |
| Digital twin and predictive maintenance | Emerging | ML, imaging, digital twins | Reliable fouling detection is now feasible | Mostly diagnostic rather than prognostic → Predictive digital twins and decision-support systems |

understanding of interactions between biofouling and submerged components [104].

The available evidence is still dominated by laboratory experiments, numerical models based on prescribed fouling conditions, settlement-panel studies, and relatively short deployment campaigns [97,98]. Experimental and CFD investigations have provided valuable estimates of biofouling-induced performance degradation, but generally require the fouling morphology, coverage, or equivalent roughness to be specified in advance [81,85]. By contrast, full-scale observations on operating tidal turbines remain comparatively rare, although the available field evidence indicates that natural colonisation can produce substantial power and thrust losses [63].

This imbalance between controlled studies and long-term operational evidence limits the validation and transferability of models describing fouling growth, hydrodynamic degradation, and lifecycle performance. Recent reviews of data-driven biofouling assessment have also identified data scarcity, inconsistent validation practices, and limited cross-site generalisation as major obstacles to predictive modelling [100,105]. Future research should therefore prioritise long-duration monitoring campaigns on commercial-scale tidal turbines, integrating biological observations, metocean conditions, hydrodynamic measurements, and turbine operational data. Such campaigns would provide the longitudinal and site-specific datasets required to establish reliable degradation trends, calibrate predictive models, and support fouling-aware maintenance planning [103,104].

Another important limitation is the absence of fully coupled predictive frameworks that integrate biological growth, hydrodynamic degradation, and techno-economic assessment. Recent reviews have highlighted that current biofouling studies are still largely compartmentalised, with biological observations, hydrodynamic modelling, monitoring, and operational decision-making often treated independently rather than within a unified lifecycle framework [103,105]. Existing approaches therefore tend to investigate isolated aspects of the problem, such as fouling growth, blade roughness effects, or maintenance strategies, without explicitly linking environmental exposure to long-term turbine performance and economic indicators. Future research should consequently focus on developing integrated multi-physics frameworks capable of coupling site-specific environmental conditions, biofouling evolution, turbine hydrodynamics, maintenance scheduling, and techno-economic metrics such as AEP and LCOE.

Table 10 highlights the current balance of the available literature by comparing the maturity of the principal research areas together with the methodologies adopted, the main findings, and the remaining knowledge gaps. The comparison shows that hydrodynamic performance

**Table 11**
Design-oriented strategies to reduce the long-term impact of biofouling on marine current turbines.

| Design choice | Biofouling benefit | Energy/LCOE implication |
|---|---|---|
| Retrievable rotor | Easier inspection and cleaning | Reduced downtime and maintenance costs |
| Smooth duct inner wall | Lower roughness-induced losses and blockages | Higher $C_P$ retention and improved AEP |
| Component-specific coatings | Greater durability under local operating conditions | Lower OPEX and longer maintenance intervals |
| Integrated sensors | Earlier fouling detection | Support for predictive maintenance strategies |
| ROV-compatible design | Easier underwater inspection and cleaning | Reduced intervention costs and improved availability |
| Reduced stagnation regions | Lower localised macrofouling accumulation | Reduced drag and improved hydrodynamic efficiency |
| Modular turbine components | Faster replacement and maintenance | Lower maintenance-related downtime |

degradation has been extensively investigated through experimental and numerical approaches, whereas predictive biofouling modelling, lifecycle techno-economic assessment, and farm-scale analyses remain comparatively underdeveloped. Future progress will therefore require stronger integration between biological observations, hydrodynamic modelling, monitoring technologies, and lifecycle analysis.

The characterisation of biofouling itself also remains insufficiently standardised. Different studies use varying roughness representations, fouling metrics, surface coverage definitions, and experimental methodologies, making quantitative comparison difficult. In particular, the relationship between biological morphology and equivalent hydrodynamic roughness remains poorly understood for marine current turbine applications [104]. Further research is therefore needed to establish standardised methodologies for fouling classification, roughness quantification, and performance-loss assessment under different operating conditions and Reynolds-number regimes.

Monitoring and detection strategies represent another significant research challenge. As tidal turbines operate in submerged, highly turbulent, and often inaccessible environments, direct inspection remains difficult and costly. Recent reviews recognise machine learning, underwater imaging, and digital-twin technologies as promising tools for predictive maintenance, but also highlight that current approaches remain largely diagnostic because of the scarcity of long-term labelled datasets and validated prognostic models [100,105]. Future developments should therefore focus on real-time monitoring systems capable of integrating sensor data, operational measurements, and image-based diagnostics to predict fouling evolution and optimise maintenance interventions before severe performance degradation occurs.

Maintenance and mitigation strategies also require further investigation. Although antifouling technologies have been extensively studied for ships and offshore structures [53], recent reviews emphasise that their transfer to tidal turbines remains poorly validated because of the substantially different hydrodynamic loading conditions and maintenance constraints [103,104]. Consequently, the long-term durability of foul-release coatings, erosion resistance under highly turbulent flows, and the effectiveness of self-cleaning mechanisms remain insufficiently understood. Further research should also evaluate the feasibility of robotic inspection, in situ cleaning, and retrieval-based maintenance through integrated operational and techno-economic analyses (Table 11).

These future-oriented strategies suggest that biofouling mitigation should progressively evolve from a purely maintenance-based approach to an integrated design-for-maintainability philosophy.

Most existing studies focus on isolated turbines, whereas the implications of biofouling at the farm scale remain largely unexplored. Although wake dynamics, farm optimisation, and array interactions have been extensively investigated for clean tidal turbines [10,11], the combined effects of biofouling-induced performance degradation on wake recovery and farm efficiency have not yet been systematically analysed. Future research should therefore investigate the coupled effects of biofouling, wake dynamics, and array optimisation for long-term commercial deployments.

Future progress in this field will require stronger integration between marine biology, hydrodynamics, materials science, monitoring technologies and techno-economic analysis. This interdisciplinary approach is essential to improve the reliability, durability and economic competitiveness of tidal energy systems under realistic offshore operating conditions.

## 5. Conclusive remarks

This review demonstrates that biofouling is a major factor limiting the long-term performance and economic viability of marine current turbines operating in harsh offshore environments. Rather than acting as a simple surface degradation mechanism, biofouling simultaneously affects hydrodynamic performance, operational reliability, maintenance requirements, and lifecycle costs. Experimental, numerical, and field studies consistently show that marine growth increases drag, alters lift characteristics, and reduces turbine efficiency, with moderate biofilm fouling generally producing limited performance penalties and severe macrofouling or calcareous growth causing substantially larger power losses.

The main finding is that biofouling should not be regarded solely as a surface roughness problem, but as a multiscale lifecycle phenomenon involving interconnected biological, hydrodynamic, operational, and techno-economic effects. Its impact depends strongly on turbine topology, operating conditions, deployment strategy, and site-specific environmental characteristics. Consequently, biofouling-induced degradation cannot be represented by universal loss factors, and lifecycle assessment requires integrated approaches linking fouling evolution, hydrodynamic response, and maintenance strategy.

The available evidence remains fragmented, since most studies rely on laboratory-scale experiments, simplified roughness representations, or short-term deployments, while long-term full-scale datasets are still scarce. This limitation motivates the integrated framework discussed in this review, which links environmental forcing, biofouling evolution, hydrodynamic degradation, monitoring, and the resulting AEP and LCOE penalties. By integrating evidence from experimental observations, hydrodynamic modelling, monitoring approaches, and techno-economic assessment, this review provides a unified perspective on the role of biofouling in the lifecycle performance of marine current turbines. The literature also indicates that effective mitigation requires a combination of antifouling coatings, adaptive operational control, inspection planning, and optimised cleaning procedures. Floating and tethered configurations may improve maintenance accessibility, but they also introduce additional submerged components exposed to marine growth. Machine learning, digital twins, and image-based monitoring offer promising support for real-time fouling assessment and predictive maintenance, although their long-term validation remains limited.

Future research should prioritise fully coupled and experimentally validated frameworks integrating marine biology, hydrodynamics, materials science, monitoring, and techno-economic assessment. Long-term full-scale campaigns and standardised fouling-characterisation methods are essential to improve model reliability and comparability. Further work is also required at farm scale to quantify fouling-induced wake changes, array-level energy losses, and maintenance optimisation under commercial operating conditions. Overall, the successful large-scale deployment of marine current turbines will depend not only on advances in energy-conversion technology, but also on the ability to predict, monitor, and mitigate biofouling-induced degradation throughout the system lifecycle.

## CRediT authorship contribution statement

**Luana Gurnari:** Writing – original draft, Methodology, Investigation, Formal analysis, Conceptualization. **Pasquale Filianoti:** Writing – review & editing, Supervision, Methodology, Conceptualization. **Domenico Coiro:** Writing – review & editing, Supervision, Methodology, Conceptualization. **Marco Torresi:** Writing – review & editing, Supervision, Methodology, Conceptualization. **Sergio Mario Camporeale:** Writing – review & editing, Supervision, Methodology, Funding acquisition, Conceptualization.

## Declaration of competing interest

The authors declare that they have no known competing financial interests or personal relationships that could have appeared to influence the work reported in this paper.

## Acknowledgements

This research has been partially funded by the Italian Ministry of University and Research under the project “SMART- Sea wave energy converters and MARine Tidal turbines - PIANO NAZIONALE DI RIPRESA E RESILIENZA (PNRR) Missione 4 “Istruzione e Ricerca” - Componente C2 Investimento 1.1, “Fondo per il Programma Nazionale di Ricerca e Progetti di Rilevante Interesse Nazionale (PRIN)”, 2022. This work has been partially funded under the National Recovery and Resilience Plan (NRRP), Mission 4, Component 2, Investment 1.3 - Call for tender No. 341 of March 15, 2022 of the Italian Ministry of University and Research, funded by the European Union - NextGenerationEU [Award Number: Network 4 Energy Sustainable Transition - NEST, Project code PE0000021, Concession Decree No. 1561 of October 11, 2022, adopted by the Italian Ministry of University and Research, CUP: D93C22000900001, Spoke2 “Energy Harvesting & Off-Shore Renewable”].

## Data availability

No data was used for the research described in the article.

## References

[1] Ahmad M, Kumar A, Ranjan R. Recent developments of tidal energy as renewable energy: an overview. River Coast Eng 2022;11:329–43.
[2] World Energy Council. World Energy Resources 2016; 2016.
[3] Kirke B, Coiro DP. Renewable energy from the oceans: from wave, tidal and gradient systems to offshore wind and solar – tidal and current energy. The Institution of Engineering and Technology; 2019. https://doi.org/10.1049/PBPO129E
[4] Hydro-Quebec. Hydro power; 2019. http://www.hydroquebec.com/data/developpementdurable/pdf/file-hydrokinetic.pdf [Accessed 26 January 2019].
[5] Charlier RH, Justus JR. Ocean energies: environmental, economic and technological aspects of alternative power sources. Amsterdam, The Netherlands: Elsevier; 1993.
[6] Selin NE. Tidal power; 2026. https://www.britannica.com/science/tidal-power [Accessed 26 January 2019].
[7] Khan MJ, Bhuyan G, Iqbal MT, Quaicoe JE. Hydrokinetic energy conversion systems and assessment of horizontal and vertical axis turbines for river and tidal applications: a technology status review. Appl Energy 2009;86(10):1823–35. https://doi.org/10.1016/j.apenergy.2009.02.017
[8] Rourke FO, Boyle F, Reynolds A. Tidal energy update 2009. Appl Energy 2010;87(2):398–409. https://doi.org/10.1016/j.apenergy.2009.08.014
[9] Zhou Z, Benbouzid M, Charpentier J-F, Scuiller F, Tang T. Developments in large marine current turbine technologies – a review. Renew Sustain Energy Rev 2017;71:852–8. https://doi.org/10.1016/j.rser.2016.12.113
[10] Yang Z, Ren Z, Li H, Pan Z, Xia W. A review of tidal current power generation farm planning: methodologies, characteristics and challenges. Renew Energy 2024;220:119603.
[11] Liu X, Lu J, Ren T, Yu F, Cen Y, Li C, Yuan S. Review of research on wake characteristics in horizontal-axis tidal turbines. Ocean Eng 2024;312:119159.
[12] Daniele E, Coiro DP. Optimization of diffuser geometry for an horizontal axis shrouded hydro turbine. In: 4th international conference on clean electrical power: renewable energy resources impact, Napoli, Italy; 2013. p. 240–7.
[13] Daniele E, Ferrauto E, Coiro DP. Horizontal axis hydroturbine shroud airfoil optimization. In: Greiner D, Galván B, Périaux J, Gauger N, Giannakoglou K, Winter G, editors. Advances in evolutionary and deterministic methods for design, optimization and control in engineering and sciences, Vol. 36 of Computational Methods in Applied Sciences. Cham: Springer; 2015. https://doi.org/10.1007/978-3-319-11541-2_15.
[14] Coiro D, Daniele E, Della Vecchia P. Diffuser shape optimization for GEM, a tethered system based on two horizontal axis hydro turbines. Int J Mar Energy 2016;13:169–79.
[15] Lazzerini G, Coiro DP, Troise G, D’Amato G. A comparison between experiments and numerical simulations on a scale model of a horizontal-axis current turbine. Renew Energy 2022;190:919–34.
[16] Riglin J, Schleicher WC, Oztekin A. Diffuser optimization for a micro-hydrokinetic turbine. In: Proceedings of the ASME 2014 international mechanical engineering congress and exposition, vol. 7. Montreal, Quebec, Canada; 2014, p. V007T09A077. https://doi.org/10.1115/IMECE2014-37304
[17] Rezek T, Camacho R, Filho N, et al. Design of a hydrokinetic turbine diffuser based on optimization and computational fluid dynamics. Appl Ocean Res 2021;107:102484.
[18] Agha A, Chaudhry HN, Wang F. Diffuser augmented wind turbine technologies: a review. Int J Renew Energy Res 2018;8(3):1369–85.
[19] Nunes MM, Brasil Junior ACP, Oliveira TF. Systematic review of diffuser-augmented horizontal-axis turbines. Renew Sustain Energy Rev 2020;133:110075. https://doi.org/10.1016/j.rser.2020.110075
[20] Vennell R. Realizing the potential of tidal currents and the efficiency of turbine farms in a channel. Renew Energy 2012;47:95–102. https://doi.org/10.1016/j.renene.2012.03.036
[21] Garrett C, Cummins P. Maximum power from a turbine farm in shallow water. J Fluid Mech 2013;714:634–43. https://doi.org/10.1017/jfm.2012.515
[22] Malki R, Masters I, Williams A, Croft TN. Planning tidal stream turbine array layouts using a coupled blade element momentum–computational fluid dynamics model. Renew Energy 2014;63:46–54.
[23] Funke SW, Kramer SC, Piggott MD. Design optimisation and resource assessment for tidal-stream renewable energy farms using a new continuous turbine approach. Renew Energy 2016;99:1046–61. https://doi.org/10.1016/j.renene.2016.07.039
[24] Paraschivoiu I. Wind turbine design with emphasis on darrieus concept. Montréal: Polytechnic International Press; 2002.
[25] Paraschivoiu I, Desy P. Aerodynamics of small-scale vertical axis wind turbines. J Propuls 1986;2.
[26] Paraschivoiu I. Double-multiple streamtube model for studying vertical-axis wind turbines. J Propuls 1988;4.
[27] Torresi M, Fortunato B, Camporeale SM. Numerical investigation of a darrieus rotor for low-head hydropower generation. In: The 3rd international conference on sustainable energy information technology, Vol. 19 of Procedia Computer Science; 2013. p. 728–35.
[28] Kumar R, Sarkar S. Effect of design parameters on the performance of helical darrieus hydrokinetic turbines. Renew Sustain Energy Rev 2022;162:112431. https://doi.org/10.1016/j.rser.2022.112431
[29] Camporeale SM, Magi V. Streamtube model for analysis of vertical axis variable pitch turbine for marine currents energy conversion. Energy Convers Manag 2000;41(16):1811–27. https://doi.org/10.1016/S0196-8904(99)00183-1
[30] Reddy KB, Bhosale AC, Saini R. Performance parameters of lift-based vertical axis hydrokinetic turbines: a review. Ocean Eng 2022;266:113089. https://doi.org/10.1016/j.oceaneng.2022.113089
[31] Pineda JC, Rubio-Clemente A, Chica E. Optimization of a gorlov helical turbine for hydrokinetic application using the response surface methodology and experimental tests. Energies 2024;17:5747. https://doi.org/10.3390/en17225747
[32] SAE renewables. https://saerenewables.com/.
[33] Strangford lough tidal turbine. https://www.power-technology.com/projects/strangford-lough/.
[34] MeyGen project. https://www.atlantisresourcesltd.com/projects/meygen/.
[35] Andritz tidal current turbines. https://www.andritz.com/products-en/marine-offshore/products/tidal-current-turbines.
[36] D10 tidal turbine ushant island. https://tethys.pnnl.gov/project-sites/d10-tidal-turbine-ushant-island.
[37] Verdant power. https://verdantpower.com/.
[38] Orbital marine power technology. https://www.orbitalmarine.com/technology/.
[39] Scotrenewables technology concept. http://www.scotrenewables.com/technology-development/the-concept.
[40] Coiro DP, Troise G, Scherillo F, De Marco A, Calise G, Bizzarrini N. Development, deployment and experimental test on the novel tethered system GEM for tidal current energy exploitation. Renew Energy 2017;114:323–36. https://doi.org/10.1016/j.renene.2017.01.040
[41] Coiro D, Troise G, Bizzarrini N, Lazzerini G, Di Noia L, Iannuzzi D, Coppola M. Design of GEMSTAR tidal current fixed pitch rotor controlled through a permanent magnet generator defluxing technique. IET Renew Power Gener. Special Issue: Selected Papers from the 7th International Conference on Clean Electrical Power 2020;14:2897–907. https://doi.org/10.1049/iet-rpg.2020.0434
[42] OpenHydro. https://www.emec.org.uk/about-us/our-tidal-clients/open-hydro/.
[43] Lunar energy tidal turbine. https://www.inference.org.uk/sustainable/17_lunar.pdf.
[44] Coiro DP, Nicolosi F, De Marco A, Melone S, Montella F. Dynamic behavior of novel vertical axis tidal current turbine: numerical and experimental investigations. In: Proceedings of international ocean and polar engineering conference; 2005, Paper No. 2005-JSC-153.

[45] Coiro D, Nicolosi F, De Marco A, Melone S, Montella F. Flow curvature effects on dynamic behaviour of a novel vertical axis tidal current turbine: numerical and experimental analysis. In: Proceedings of OMAE2005: 24th international conference on offshore mechanics and arctic engineering, Halkidiki, Greece; 2005, OMAE2005-67193.
[46] EMEC tidal developers. https://www.emec.org.uk/marine-energy/tidal-developers/.
[47] Gorlov A. Development of the helical reaction hydraulic turbine. Tech. rep. Boston: Northeastern University; 1998.
[48] Moreau M, Germain G, Maurice G, Richard A. Sea states influence on the behaviour of a bottom mounted full-scale twin vertical axis tidal turbine. Ocean Eng 2022;265:112582. https://doi.org/10.1016/j.oceaneng.2022.112582
[49] OceanQuest. https://www.hydroquest.fr/en/oceanquest-en/.
[50] Blue energy. http://www.bluenergy.com/index.html.
[51] Minesto. https://minesto.com/.
[52] Yebra DM, Rasmussen SN, Weinell C, Pedersen LT. Marine fouling and corrosion protection for off-shore ocean energy setups. In: Proceedings of the 3rd international conference on ocean energy, Bilbao; 2010.
[53] Yebra DM, Kiil S, Dam-Johansen K. Antifouling technology: past, present and future steps towards efficient and environmentally friendly antifouling coatings. Prog Org Coat 2004;50:75–104. https://doi.org/10.1016/j.porgcoat.2003.06.001
[54] Wang Z, Wang X, Huang Y, Zhou H, Wu Y, Sun Y, Nan Y, Xu H, Pu J, Hou B. Macrofouling organisms: protection or damage of steel in marine environments? Corros Sci 2023;212:110928.
[55] Degraer S, Carey DA, Coolen JWP, Hutchison ZL, Kerckhof F, Rumes B, Vanaverbeke J. Offshore wind farm artificial reefs affect ecosystem structure and functioning: a synthesis. Oceanography 2020;33(4):48–57. https://doi.org/10.5670/oceanog.2020.405
[56] Hunsucker KZ, Gardner H, Lieberman K, Swain G. Using hydrodynamic testing to assess the performance of fouling control coatings. Ocean Eng 2019;194:106677.
[57] Suleiman OME, Ali SMS. Introduction and literature review of corrosion and biofouling in marine environment. Int J Eng Appl Sci Technol 2022;7(8):41–61.
[58] Vinagre PA, Simas T, Cruz E, Pinori E, Svenson J. Marine biofouling: a European database for the marine renewable energy sector. J Mar Sci Eng 2020;8:495. https://doi.org/10.3390/jmse8070495
[59] Wahl M. Marine Epibiosis. I. fouling and antifouling: some basic aspects. Mar Ecol Prog Ser 1989;58:175–89.
[60] Almeida LP, Coolen JWP. Modelling thickness variations of macrofouling communities on offshore platforms in the Dutch north sea. J Sea Res 2020;156:1–8.
[61] Cao S, Wang J, Chen H, Chen D. Progress of marine biofouling and antifouling technologies. Chin Sci Bull 2011;56:598–612.
[62] Miller RG, Macleod AK. Marine growth mapping and monitoring: feasibility of predictive mapping of marine growth. Tech. Rep. PN000111-SRT-001 Glasgow, UK: Offshore Renewable Energy Catapult; 2016.
[63] Starzmann R, Kaufmann N, Jeffcoate P, Pieroway R, Guerra M, Hay A. Effect of fouling on the performance of an instream turbine. Int Mar Energy J 2022;5(3):229–37. https://doi.org/10.36688/imej.5.229-237
[64] Song S, Shi W, Demirel YK, Atlar M. The effect of biofouling on the tidal turbine performance. In: Applied energy symposium. Boston, MA, USA: Massachusetts Institute of Technology; 2019.
[65] Leask marine ticks another tidal decommissioning job off to-do list. https://www.offshore-energy.biz/leask-marine-ticks-another-tidal-decommissioning-job-off-to-do-list/.
[66] Tidal energy turbine removal. http://www.racerocks.ca/tidal-energy-turbine-removal/.
[67] Demirel Y, Uzun D, Zhang Y, Fang HC, Day A, Turan O. Effect of barnacle fouling on ship resistance and powering. Biofouling 2017;33:819–34. https://doi.org/10.1080/08927014.2017.1373279
[68] Owen D, Demirel YK, Oguz E, Tezdogan T, Incecik A. Investigating the effect of biofouling on propeller characteristics using CFD. Ocean Eng 2018. https://doi.org/10.1016/j.oceaneng.2018.01.087
[69] Farkas A, Degiuli N, Martić I. The impact of biofouling on the propeller performance. Ocean Eng 2021;219:108376. https://doi.org/10.1016/j.oceaneng.2020.108376
[70] Amiruddin W, Hakim ML, Firdhaus A, Purnamasari D, Tuswan T, Samuel S, Mursid O. Prediction of the impact of biofouling roughness on a full-scale planing boat performance using CFD. Ocean Eng 2024;301:117457.
[71] Song S, Demirel YK, Atlar M. An investigation into the effect of biofouling on full-scale propeller performance using CFD. In: Proceedings of the ASME 2019 38th international conference on ocean, offshore and arctic engineering, Glasgow, Scotland, UK; 2019.
[72] Song S, Demirel YK, Atlar M. Penalty of hull and propeller fouling on ship self-propulsion performance. Appl Ocean Res 2020;94:102006. https://doi.org/10.1016/j.apor.2019.102006
[73] Coraddu A, Lim S, Oneto L, Pazouki K, Norman R, Murphy AJ. A novelty detection approach to diagnosing hull and propeller fouling. Ocean Eng 2019;176:65–73. https://doi.org/10.1016/j.oceaneng.2019.01.054
[74] Uzun D, Sezen S, Atlar M, Turan O. Effect of biofouling roughness on the full-scale powering performance of a submarine. Ocean Eng 2021;238:109773.
[75] Song S, Demirel YK, Atlar M, Shi W. Prediction of the fouling penalty on the tidal turbine performance and development of its mitigation measures. Appl Energy 2020;276:115498. https://doi.org/10.1016/j.apenergy.2020.115498
[76] Farkas A, Degiuli N, Martić I, Ančić I. Performance prediction method for fouled surfaces. Appl Ocean Res 2020;99:102151.
[77] Uzun D, Sezen S, Ozyurt R, Atlar M, Turan O. A CFD study: influence of biofouling on a full-scale submarine. Appl Ocean Res 2021;109:102561.
[78] Gurnari L, Filianoti P, Coiro D, Camporeale SM. On the design of a scaled rotor for a tethered tidal converter to deploy at sea. J Phys Conf Ser 2024;2893(1):012020.
[79] Alizzio D, Gurnari L, Nardi V, Torresi M, Coiro D, Filianoti P, Camporeale S. On the design of a small scale tidal converter for long time deployment at sea. In: Proceedings of the European wave and tidal energy conference, Vol. 15; 2023.
[80] Coiro DP, Maisto U, Scherillo F, Melone S, Grasso F. Horizontal axis tidal current turbine: numerical and experimental investigations. In: OWEMES 2006, Civitavecchia, Italy; 2006.
[81] Walker JM, Flack KA, Lust EE, Schultz MP, Luznik L. Experimental and numerical studies of blade roughness and fouling on marine current turbine performance. Renew Energy 2014;66:257–67. https://doi.org/10.1016/j.renene.2013.12.012
[82] Priegue L, Stoesser T. The influence of blade roughness on the performance of a vertical axis tidal turbine. Int J Mar Energy 2017;17:136–46. https://doi.org/10.1016/j.ijome.2017.01.009
[83] Walker JS, Green RB, Gillies EA, Phillips C. The effect of a barnacle-shaped excrescence on the hydrodynamic performance of a tidal turbine blade section. Ocean Eng 2020;217:107849. https://doi.org/10.1016/j.oceaneng.2020.107849
[84] Afshar O. Assessing the long-term performance of tidal turbines subject to biofouling [Ph.D. thesis]. University of Tasmania; 2019.
[85] Farkas A, Degiuli N, Martić I, Barbarić M, Guzović Z. The impact of biofilm on marine current turbine performance. Renew Energy 2022;190:584–95. https://doi.org/10.1016/j.renene.2022.03.134
[86] Farkas A, Degiuli N, Martić I. Towards the prediction of the effect of biofilm on the ship resistance using CFD. Ocean Eng 2018;167:169–86.
[87] Rashid H, Benbouzid M, Amirat Y, Berghout T, Titah-Benbouzid H, Mamoune A. Biofouling detection and classification in tidal stream turbines through soft voting ensemble transfer learning of video images. Eng Appl Artif Intell 2024;138:109316.
[88] Löschau M, Krätke R. Efficacy and toxicity of self-polishing biocide-free antifouling paints. Environ Pollut 2005;138:260–7. https://doi.org/10.1016/j.envpol.2005.04.015
[89] Korkut E, Atlar M. An experimental investigation of the effect of foul release coating application on performance, noise and cavitation characteristics of marine propellers. Ocean Eng 2012;41:1–12. https://doi.org/10.1016/j.oceaneng.2011.12.012
[90] Candries M. Drag, boundary-layer and roughness characteristics of marine surfaces coated with antifoulings [Ph.D. thesis]. University of Newcastle upon Tyne; 2001.
[91] Khor YS, Xiao Q. CFD simulations of the effects of fouling and antifouling. Ocean Eng 2011;38(10):1065–79.
[92] Candries M, Atlar M. The measurement of the drag characteristics of tin-free self-polishing co-polymers and fouling release coatings using a rotor apparatus. Biofouling 2003;19(1):27–36 (Suppl. 1).
[93] García S, Trueba A, Boullosa-Falces D, Islam H, Soares CG. Predicting ship frictional resistance due to biofouling using Reynolds-averaged Navier-Stokes simulations. Appl Ocean Res 2020;101:102203.
[94] Tang Y, Wu X, Zou S, Qin H, Sun K, Sun L, Hou J, Shi W, Li C, Guo F. Resorcinol–formaldehyde resin combining epoxy resin as composite coating with efficient anti-corrosion resistance and anti-biofouling capacity. Prog Org Coat 2025;203:109177.
[95] Bressy C, Lejars M. Marine fouling: an overview. J Ocean Technol 2014;9(4).
[96] Callow JA, Callow ME. Marine biofouling: a sticky problem. Biologist 2002;49:1–4.
[97] Want A, Bell MC, Harris RE, Hull MQ, Long CR, Porter JS. Sea-trial verification of a novel system for monitoring biofouling and testing anti-fouling coatings in highly energetic environments targeted by the marine renewable energy industry. Biofouling 2021;37(4):433–51. https://doi.org/10.1080/08927014.2021.1928091
[98] Want A, Porter JS. BioFREE: an international study of biofouling impacts on the marine renewable energy industry. In: OCEANS 2018 MTS/IEEE Kobe Techno-Oceans; 2018. p. 1–7. https://doi.org/10.1109/OCEANSKOBE.2018.8559322
[99] Nall CR, Schläppy M-L, Cottier-Cook EJ, Guerin AJ. Influence of coating type, colour, and deployment timing on biofouling by native and non-native species in a marine renewable energy context. Biofouling 2022;38(7):1–17. https://doi.org/10.1080/08927014.2022.2121209
[100] Rashid H, Benbouzid M, Titah-Benbouzid H, Amirat Y, Mamoune A. Tidal stream turbine biofouling detection and estimation: a review-based roadmap. J Mar Sci Eng 2023;11:908. https://doi.org/10.3390/jmse11050908
[101] Aldersey-Williams J, Rubert T. Levelised cost of energy – a theoretical justification and critical assessment. Energy Policy 2019;124:169–79. https://doi.org/10.1016/j.enpol.2018.10.004
[102] Guo C, Sheng W, De Silva DG, Aggidis G. A review of the levelized cost of wave energy based on a techno-economic model. Energies 2023;16(5):2144. https://doi.org/10.3390/en16052144
[103] Loxton J, Macleod AK, Nall CR, McCollin T, Machado I, Simas T, Vance T, Kenny C, Want A, Miller RG. Setting an agenda for biofouling research for the marine renewable energy industry. Int J Mar Energy 2017;19:292–303. https://doi.org/10.1016/j.ijom7.08.006
[104] Portas A, Briand J-F, Damblans G, Quillien N. A review of biofouling characteristics and issues for offshore renewable energy industry. Biofouling 2026;42(4):339–60. https://doi.org/10.1080/08927014.2026.2630946
[105] Hasil SD, Zahid Z, Michailides C, Shi W, Irshad F. A review on machine learning and bioinformatics to study biofouling in marine renewable energy devices: modeling, performance prediction, and maintenance planning. J Mar Sci Eng 2026;14(6):549. https://doi.org/10.3390/jmse14060549